Clearing the Fungal FoG: Perseverance, a property distinct from resistance, is associated with clinical persistence

Alexander Rosenberg[1*], Iuliana V. Ene[2*], Alon M. Dahan[1], Ella Shtifman Segal[1], Arnaldo L. Colombo[3], Richard J. Bennett[2], Judith Berman[1]**

1. School of Molecular Cell Biology and Biotechnology, Tel Aviv University, Ramat Aviv Israel
2. Department of Molecular Microbiology and Immunology, Brown University, Providence, Rhode Island, USA
3. Department of Medicine, Federal University of São Paulo, São Paulo, Brazil

*Equal contributions

**Corresponding Author: judithberman11@gmail.com, +972-52-584-2031

Abstract

Drug resistance, defined by the minimal inhibitory concentration (MIC), often does not predict whether fungal infections will respond to drug treatment in the clinic. Here we define and quantify an antifungal response, termed '*perseverance'*, that correlates with clinical outcomes in patients treated with fluconazole, the most widely used antifungal drug. Perseverance is defined by the ability of fungal cells to grow at drug concentrations above the MIC, and is measured either as the 'fraction of growth' (FoG) in drug disk diffusion assays, or as the degree of 'supra-MIC growth' (SMG) in broth microdilution assays. Perseverance is distinct from resistance and is related to the proportion of cells that form colonies at supra-MIC drug concentrations. Higher perseverance correlates with shorter lag times at high drug concentrations, highlighting a critical distinction from 'tolerance' in bacterial populations. Importantly, several adjuvant drugs, including inhibitors of Hsp90 and calcineurin, eliminate perseverance without altering the MIC. We also find that perseverance and resistance are sensitive to mutations in different pathways, underscoring the distinct nature of the two phenomena. Analysis of isolates recovered from clinically persistent or non-persistent infections in immunocompetent patients reveals that persistent isolates show higher levels of perseverance than isolates cleared by antifungals. Thus, perseverance is an intrinsic property of fungal isolates that correlates with the success or failure of treatment in the clinic, and may provide a useful parameter for predicting clinical persistence and choosing appropriate antifungal therapies.

Introduction

Antimicrobial drug resistance, the ability to grow well at high drug concentrations irrespective of treatment duration, involves several distinct mechanisms including alteration in drug targets, drug efflux or drug inactivation. Of note, infections generally follow the “90/60” rule for predicting therapeutic outcomes based on *in vitro* susceptibility testing: approximately 90% of susceptible isolates and 60% of resistant isolates respond to therapy[1-5]. This is important as it implies that drug resistance, as defined by *in vitro* assays, is often not sufficient to explain clinical outcomes, and that effective treatment is likely influenced by patient attributes as well as by additional characteristics of the infecting isolates.

Two microbial variables that have been established to affect drug responses in bacteria are “tolerance” and “persistence”. Importantly, both tolerant and persistent isolates require similar levels of antibiotic drugs for killing as susceptible isolates. However, the duration of drug treatment necessary to achieve killing of tolerant or persistent strains is much longer than that necessary for susceptible strains. Mechanistically, both tolerance and persistence involve the ability of cells to survive and/or grow during transient exposure to high drug concentrations. Toxin/antitoxin-modules are responsible for promoting tolerance and persistence in some cases, and isolates with more toxin/antitoxin modules therefore tend to exhibit higher levels of persistence[6]. A major distinction between the two phenomena is the size of the subpopulations involved: tolerance is observed in 10-90% of cells whereas persistence occurs in <1% of cells (reviewed in[7])., Both tolerance and persistence typically involve slower growth or a longer lag phase, which effectively reduces metabolism and toxicity of the drug in the exposed cells. This is reflected in the minimum duration for killing (MDK), a quantitative parameter which is useful for studying cidal, but not static, drug responses[7-9].

The term “tolerance” has been discussed for fungal isolates, and is loosely defined as survival above intrinsic inhibitory concentration levels. Currently, the most widely used antifungal drugs are azoles, which interact with sterols in the fungal membrane. Azoles are

primarily fungistatic in *Candida albicans*, one of the most prevalent human fungal pathogens. With respect to fungistatic drugs, tolerance is likely synonymous with “trailing growth”, defined as the residual growth of cells at high antifungal concentrations in liquid cultures, and which has been detected in a subset of clinical isolates[10-16]. Tolerance has been proposed to promote the appearance of ‘persister cells’ that can cause recurrent infections[16], although this has not been demonstrated. Strains that showed evidence of trailing growth did not have a clear difference in virulence in a systemic model of candidiasis[17-19] or in short term responses to antifungal treatments in HIV patients[20]. It is currently unclear whether trailing growth impacts the clinical outcome of infections by *Candida* species, yet 25-60% of isolates show some evidence of trailing growth[21-23]. However, conventional susceptibility assays have been optimized to avoid detection of trailing growth[25,26] by determining the MIC at 18-24 h, at which time the trailing effect is minimal or absent[24,27]. Nonetheless, we posit that both tolerance and trailing growth yield increased numbers of cells dividing for long periods of time in the presence of antifungals, and can potentially alter the ability to adapt in the patient, a property termed “clinical persistence”.

C. albicans is a diploid species that lacks meiosis and thus relies on mitotic processes and a parasexual cycle for genetic variation[28-30]. Each individual largely carries their own strain, often inherited from their mother, with isolates from different patients exhibiting broad divergence illustrated by thousands of unique SNPs[31-34]. There are currently only four classes of approved antifungal drugs, and combination therapy using antifungals together with adjuvant drugs is considered a promising route to extend the effectivity of current antifungals[15,46-50]. Resistance to fluconazole, the most widely used fungistatic drug, is an increasing problem in the clinic and is generally driven by increased drug efflux and/or changes in ergosterol biosynthesis, the target of azole drugs[39]. A broad range of adjuvant drugs have been reported to enhance the activity of fluconazole, with inhibitors of Hsp90 and calcineurin the most prominent among them[40,41]. Targeting Hsp90, a highly abundant chaperone, or its client protein calcineurin, has

been proposed as a “powerful, broadly effective therapeutic strategy for fungal infectious disease”[54].

In the clinic, persistence refers to a subset of infections that do not respond to drug treatment despite the infecting isolate being drug susceptible when evaluated *in vitro*. Host immune status may play a key role in determining the persistence or recurrence of fungal infections[59-61]. However, in the absence of host immune deficiencies or drug resistant isolates, it is unclear to what extent the intrinsic properties of fungal isolates impact clinical persistence. Strain diversity is an important parameter that is often overlooked in laboratory studies of antifungal responses. There are multiple major and minor clades of *C. albicans*[35-37] and some exhibit clade-specific levels of susceptibility to specific antifungals[38]. Clinical persistence of *C. albicans* has been observed in many patients, with particularly high incidence rates in neonates[62-64]. The inability to clear infection is associated with increased mortality; in one study the case-fatality rate was 54% among infections with persistent candidemia and only 3% among those with non-persistent candidemia[65]. The mechanisms underlying *C. albicans* clinical persistence have yet to be defined and it is not understood how fungal infections can persist in the bloodstream despite having MIC levels that indicate they should be effectively cleared by antifungal treatment.

We set out to characterize drug-response variables that could influence clinical persistence of fungal infections and be generalizable across all *C. albicans* clades. This work utilized an image analysis pipeline, *diskImageR*, for quantitative examination of disk diffusion assays (DDAs)[66]. This approach examines both the radius (RAD) of the zone of inhibition (ZOI), a parameter that correlates with the MIC, as well as the fraction of growth (FoG) within the ZOI, a parameter that correlates with ‘trailing growth’ or ‘tolerance’[10,15,67-70]. We emphasize that FoG is an independent variable that does not correlate with MIC[66] or with *C. albicans* clade distinctions[23]. We characterized FoG in disk diffusion assays and its equivalent, supra-MIC growth (SMG), in broth microdilution assays (BMDAs), and demonstrated that the two

parameters correlate with one another and that they provide a measure of what we term '*perseverance'*. Perseverance correlates with the proportion of cells in the population that can grow at high drug concentrations. Strains with high perseverance show a shorter lag phase following drug exposure, in contrast to what is observed for bacterial tolerance to cidal drugs[7]. Surprisingly, inhibitors of Hsp90 and of calcineurin eliminated perseverance completely but did not affect the MIC in any of the >50 isolates tested. Importantly, we found that perseverance was significantly higher in clinically-persistent isolates of *C. albicans* than in those readily cleared by fluconazole treatment, thereby providing support for the idea that perseverance is a parameter with clinical implications.

Results

Slow, supra-MIC growth is distinct from resistance

C. albicans isolates display high genotypic and phenotypic variability, including distinct responses to antifungal drugs. We examined the responses of isolates from different genetic backgrounds and types of infections to some of the most frequently used antifungals drugs using *diskImageR,* a quantitative disk diffusion assay analysis tool. *diskImageR* can quantify two parameters: the radius of the zone of inhibition (ZOI) at 20% inhibition (RAD_{20}) as an indicator of susceptibility/resistance; and the fraction of growth within the ZOI (FoG_{20}), calculated as the area under the curve relative to the maximum possible area[66] (Fig. 1A). A screen of 219 clinical isolates (Supplementary Table 1), revealed that FoG levels on fluconazole (FLC) range from 0.10 to 0.85 and do not correlate with RAD_{20} levels (Fig. 1B,C), indicating that RAD and FoG measure two independent responses to this drug.

We selected a set of seven isolates to represent the breadth of diversity among clinical isolates for further characterization of FoG and the growth parameters associated with it (Fig. 1C, colored data points). We note that for drug-resistant strains such as T101 (MIC = 64, Supplementary Fig. 2A), the very small ZOI makes FoG measurements less accurate. For a

given isolate, both FoG and RAD levels were reproducible when evaluating cells taken from different colonies or when cells were taken from inside or outside the ZOI and re-tested for their drug responses (Fig. 1D). These observations indicate that FoG, the level of growth inside the ZOI, is a stable and heritable property of a given *C. albicans* strain. Moreover, cells growing within the ZOI are not drug resistant and yield progeny indistinguishable from the rest of the cells in the population.

FoG and RAD levels exhibited different dynamics in the disk diffusion assays. While RAD levels were constant after 24 h, FoG was often undetectable at 24 h and only became fully apparent at 48 h (Fig. 1E). Thus, the detection of RAD is generally time-independent while the detection of FoG is largely time-dependent. By definition, drug susceptibility is a concentration-dependent parameter and, as expected, when drug concentration in the disk was increased, the ZOI size (and thus RAD) also increased (Fig. 1F, Supplementary Table 1). In contrast, FoG levels were similar irrespective of the drug concentration in the disk, indicating that this drug response is concentration-independent. Taken together, these results highlight the distinctive nature of the drug response measured as FoG, which is more reminiscent of the clinically ignored trailing effect, and is different from classical MIC measurements.

A range of FoG levels also was detectable with different antifungal drugs including other azoles (posaconazole and ketoconazole), 5-fluorocytosine and, albeit to a lesser degree, echinocandins (micafungin and caspofungin) and polyenes (amphotericin B) (Supplementary Fig. 1A). Overall, FoG levels were generally lower in response to drugs considered to be fungicidal (e.g., echinocandins and polyenes) rather than fungistatic (e.g., azoles, 5-fluorocytosine). We also measured drug responses in different fungal species including *C. tropicalis, Candida krusei, Candida glabrata, Candida parapsilosis* and *S. cerevisiae,* resulting in a range of RAD and FoG levels to each of the antifungals tested (Supplementary Fig. 1B). *C. parapsilosis* exhibited the highest susceptibility to azoles (highest RAD) with intermediate FoG levels. In response to azoles, *C. glabrata* exhibited the highest FoG levels (but intermediate

Figure 1

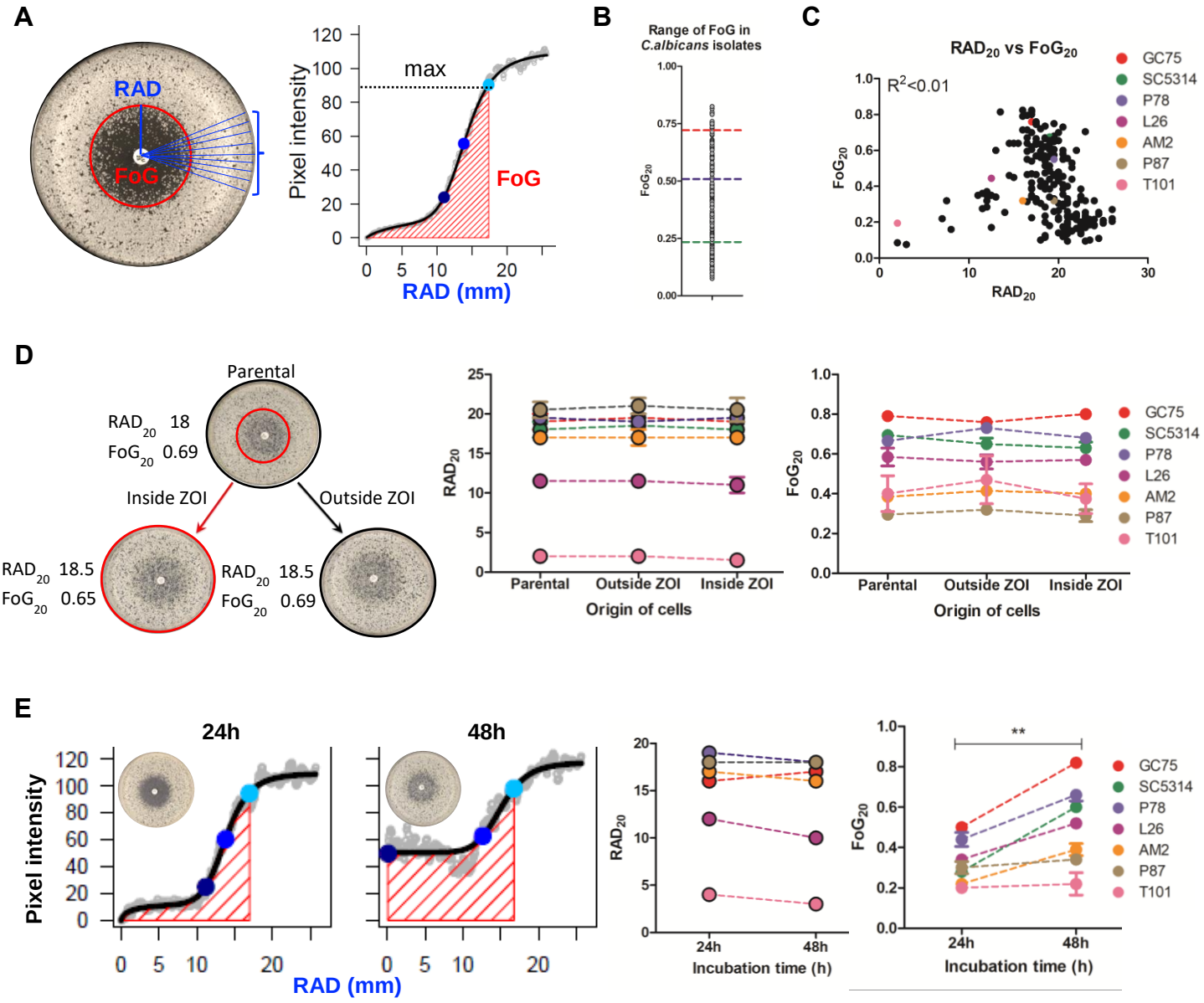
A
RAD
FoG
max
Pixel intensity
RAD (mm)
B
Range of FoG in C.albicans isolates
FoG20
C
RAD20 vs FoG20
R2<0.01
FoG20
RAD20
GC75
SC5314
P78
L26
AM2
P87
T101
D
Parental
RAD20 18
FoG20 0.69
Inside ZOI
Outside ZOI
RAD20 18.5
FoG20 0.65
RAD20 18.5
FoG20 0.69
RAD20
FoG20
Parental
Outside ZOI
Inside ZOI
Origin of cells
E
24h
48h
Pixel intensity
RAD (mm)
RAD20
FoG20
Incubation time (h)
**
F
FLC conc 25 µg 50 300 µg
RAD20 19 21 23
FoG20 0.65 0.64 0.64
RAD20
FoG20
FLC concentraion on disk (µg)

Figure 1. Measuring drug responses of *C. albicans* clinical isolates in disk diffusion assays (DDAs).
(a) Illustration of *diskImageR* analysis, which measures pixel intensity corresponding to cell density, along 72 radii every 5°. The average radius (RAD) threshold is the distance in mm corresponding to the point where 20%, 50% or 80% growth reduction occurs (light, medium, dark blue dots). The Fraction of Growth inside the ZOI (FoG) is the area under the curve (red hatched area) at the RAD threshold level, divided by the maximum area proscribed by the RAD threshold (max). (b) Range of FoG levels in 219 *C. albicans* clinical isolates (from Dr. R. Ben-Ami). Red, blue and green lines estimate high, medium and low levels of FoG respectively. Unless otherwise specified, DDAs were performed using a single 25 µg fluconazole disk analyzed after 48h at 30°C. (c) Comparison of FoG_{20} and RAD_{20} for the 219 isolates (*P*- 0.0064,n=219). (d) RAD_{20} and FoG_{20} for a parental strain and progeny colonies picked from inside and outside the ZOI. Left panel, DDAs for strain SC5314, and corresponding RAD (middle, black outlined dots) (One way ANOVA, *P*- 0.99, n groups- 3 , *F*- 0.0032) and FoG (right, dots without outlines) (One way ANOVA, *P*- 0.97, n groups- 3 , *F*- 0.029) levels for diverse *C. albicans* isolates (corresponding to indicated colors)
(e) Effect of incubation time on RAD and FoG values. Left panel, illustration of *diskImageR* analysis at 24 h and 48 h; corresponding RAD (middle panel) (Paired t-test, P- 0.094, t=2, df=6,n pairs-7) and FoG (right panel) levels (Paired t-test, P- 0.0071, t=4, df=6,n pairs-7) for strains as in (d)
(f) RAD is concentration-dependent and FoG is concentration independent as measured with disks containing increasing concentrations of fluconazole (25, 50 and 300 µg fluconazole) for strain SC5314 (left panel); corresponding RAD (middle panel) and FoG (right panel) levels for strains as in (d).

RAD), followed by *C. tropicalis* and *C. krusei.* We posit that the high FoG levels of *C. glabrata* could contribute to the high incidence of azole resistance and to the intrinsic low susceptibility of the species to this class of antifungals[71-73]. Most *S. cerevisiae* strains displayed low FoG levels in response to azoles, but had intermediate FoG levels on echinocandins and polyenes. Clearly, FoG is a property observed in a range of yeast species and is not specific to fluconazole.

Broth microdilution assays (BMDAs) are considered the clinical assay of choice for quantifying drug susceptibility. We therefore measured MIC_{50} values, the lowest drug concentration that inhibits 50% of growth, in the seven *C. albicans* isolates chosen above. Trailing growth is frequently observed in BMDAs as increased growth at 48 h relative to 24 h, but this phenomenon is not usually quantified or otherwise used in clinical assays. We quantified supra-MIC growth (SMG) in BMDAs as the average growth per well (at 48 h) above the MIC_{50} (at 24 h) normalized to growth levels in the absence of drug (Fig. 2A). Using this parameter, most isolates exhibited growth at drug concentrations above the MIC, while the MIC levels did not change between 24 and 48 h. Thus, SMG provides a parameter that quantifies the trailing growth effect and is independent of resistance/MIC. Furthermore, SMG, like FoG, is dependent upon longer assay times and is more readily detectable at 48 h rather than 24 h (Fig. 2B,C). Similar to FoG, cells taken from wells above or below the MIC_{50} were indistinguishable from parental cells when re-analyzed for MIC and SMG levels (Supplementary Fig. 2A). Analysis of the relationship between parameters measured in BMDAs and DDAs revealed that SMG and FoG correlate well ($R^2 = 0.82$, $P < 0.01$, n – 12, Supplementary Fig. 2B), whereas there was no relationship between SMG and MIC ($R^2 = 0.25$, $P < 0.01$, n – 28 Supplementary Fig. 2B). **This indicates that FoG and SMG reflect similar features of growth at supra-MIC antifungal concentrations, and that this response is independent from drug resistance**. Of note, BMDAs cannot detect the individual sub-populations that are detectable on agar

Figure 2

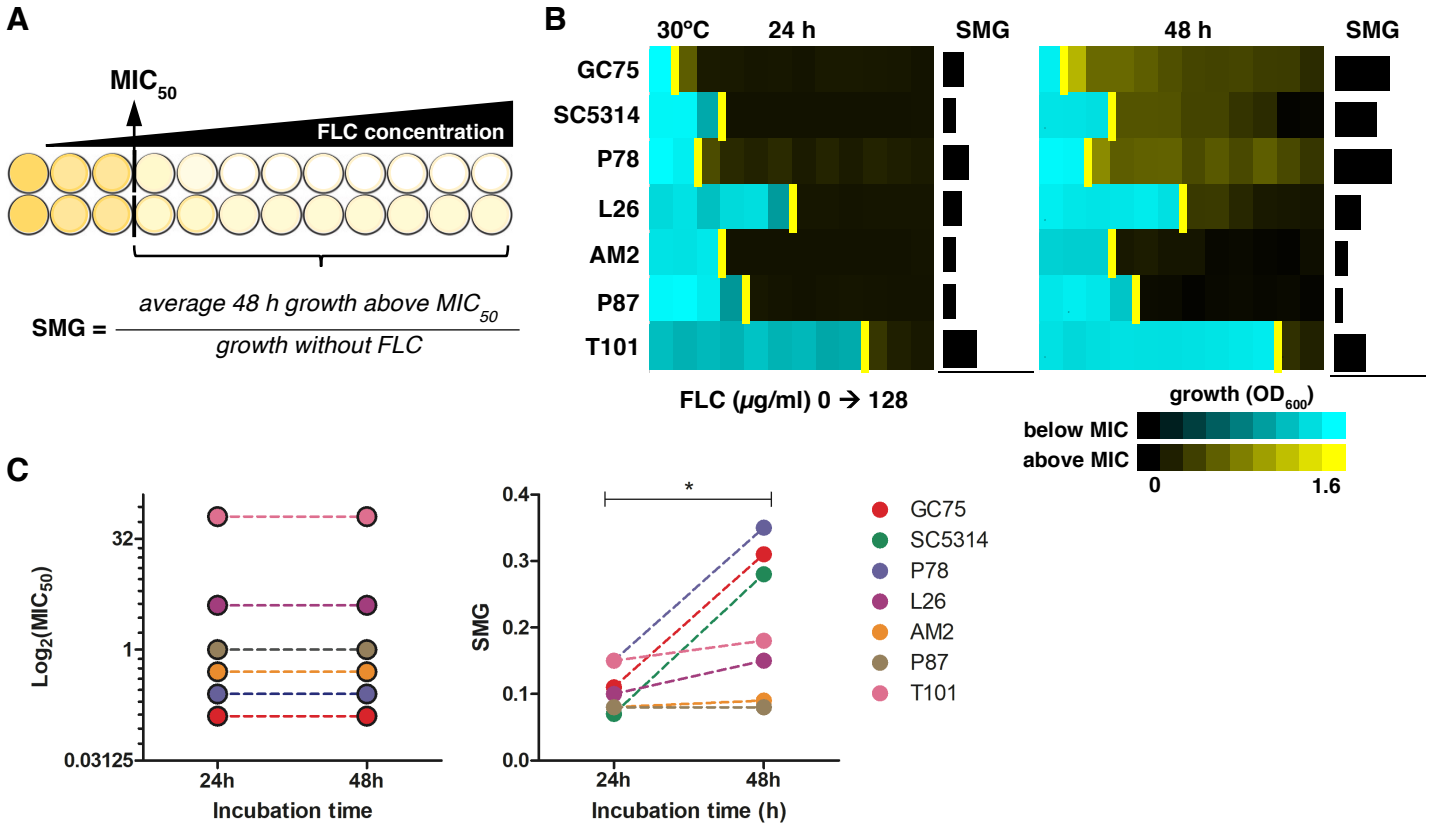

Figure 2. Measuring drug responses of *C. albicans* clinical isolates in liquid broth assays. (a) Illustration of MIC and Supra-MIC Growth (SMG) calculations. MIC values were calculated at 24 h as the fluconazole concentration at which 50% of the growth in the absence of fluconazole is inhibited. Supra-MIC Growth (SMG) was calculated as the average growth per well above the MIC divided by the level of growth in the well without drug. fluconazole was used in two-fold dilutions (0, 0.125, 0.25, 0.5, 1, 2, 4, 8, 16, 32, 64, and 128 μg/ml). (b) Heatmaps illustrating OD_{600} levels for concentrations above the MIC (yellow bar) in cyan and beyond the MIC in yellow for the same seven *C. albicans* isolates from Fig. 1. Maps show OD_{600} at 24 and 48 h. (c) Corresponding MIC (t-test, *P*=1,t=0, df=6, n pairs=7) and SMG (t-test, *P*=0.0356 ,t=2.7, df=6, n pairs=7) levels for these strains measured at 24 and 48 h.

medium and thus are more prone to jackpot events (overrepresentation of rare mutants with a selective growth advantage).

Growth characteristics of FoG and SMG

Different environmental cues that influence trailing growth include temperature, pH, carbon source and the type of surface cells are growing on[25,26,67]. Similarly, we found that FoG and SMG levels were influenced by different growth conditions. For example, FoG and SMG levels were reduced significantly at pH 4.5 relative to pH 7, albeit to different degrees in different strains (Supplementary Fig. 3A,B). Most clinical MIC assays are performed at 37°C, while laboratory assays are often performed at lower temperatures (30°C) to avoid confounding morphologies such as filamentous growth. Temperatures above 30°C had little effect on RAD and MIC levels but had a significant impact on both FoG and SMG, and this effect was dependent on strain background (Supplementary Fig. 3C,D). *C. albicans* isolates were very sensitive to the shift from 30°C to 37°C, but did not display significant differences in either FoG or SMG between 37°C and 39°C/41°C (Supplementary Fig. 3C,D), suggesting that the shift from normal body temperature to febrile temperature does not necessarily alter drug responses. In addition, DDAs performed using rich medium (YPD) often gave slightly different FoG and RAD levels than those using casitone medium (Supplementary Fig. 3E). Nonetheless, the relative differences between the degree of FoG in different *C. albicans* strains was generally maintained between the two media (Supplementary Fig. 3E).

Growth properties of cells withstanding supra-MIC drug concentration

To characterize the growth properties of cells underlying the FoG/SMG response, we measured the growth of individual colonies inside the ZOI. All strains exhibited nearly 100% viability in the presence of drug relative to growth in the absence of drug despite having a broad range of FoG/SMG levels (Fig. 3A). This result is consistent with the fungistatic nature of fluconazole and illustrates that neither FoG nor SMG is a measure of cell viability.

We next measured the proportion of the population that formed colonies at supra-MIC drug concentrations. The number of colonies that grew on 10 µg/ml fluconazole (a concentration 10-20-fold above the MIC of the average strain) ranged between 25% and 98% and correlated well with FoG levels on DDAs (Fig. 3B, $R^2 = 0.91$, $P < 0.01$, n=11). This indicates that FoG is due to having a relatively large subpopulation of cells that is able to grow, albeit slowly, at supra-MIC drug concentrations.

We turned to time-lapse microscopy to follow the dynamics of early cell growth in the presence of 10 µg/ml fluconazole. As expected from previous studies[29], exponentially growing cells plated onto supra-MIC drug concentrations did not immediately stop growing in the presence of fluconazole. Rather, the majority of cells continued dividing for ~4-6 h, and then divided more slowly to different degrees (Fig. 3C and Supplementary videos 1-3). Isolates with low FoG (e.g., P87) generally formed fewer growing microcolonies over a 24 h period than those with high FoG (e.g., SC5314, Fig. 3C) (similar numbers of cells were plated in each well). Thus, analysis of early cell growth, before colonies were detectable on plates, reflected the two trends seen with assays that measure visible colony growth: higher FoG isolates had shorter time of colony appearance (Fig. 3E) and greater number of cells growing on supra-MIC drug concentrations (Figs. 3B).

We next measured the dynamics of colony growth in the presence of supra-MIC drug concentrations (10 µg/ml fluconazole) using *ScanLag,* an assay that measures growth parameters with a flatbed scanner and colony size image analysis (Fig. 3D). *ScanLag* records the initial time of colony appearance (ToA, a proxy for lag phase length), the area occupied by light pixels (a proxy for colony size), and the change in this area over time (a measure of growth rate)[75]. Studies of tolerance in bacteria with *ScanLag* revealed that tolerant strains have longer ToA (lag times), a property thought to facilitate their survival[76]. We adapted *ScanLag* for use with *C. albicans* and applied it to a series of isolates spanning a range of FoG/SMG levels (Fig. 3E and Supplementary Fig. 4). In the absence of drug, ToA values differed across the set of

isolates, indicating that ToA is a strain-specific parameter which reflects the genetic diversity of the isolates used. As expected, ToA was longer in the presence of supra-MIC drug concentrations (10 µg/ml fluconazole) than in medium without drug, except for truly resistant strains (Fig. 3E). High FoG isolates formed visible colonies ~10 h faster than low FoG isolates (Fig. 3E). This suggests that high FoG strains can overcome the inhibitory pressures of the antifungal more efficiently than low FoG strains. Of note, ToA was the only *ScanLag* parameter found to be associated with FoG; neither colony growth rate nor final colony size correlated with FoG/SMG levels (Fig. 3F and Supplementary Fig. 5A,B).

We performed a parallel analysis examining perseverance in two additional lineages that included strains with differences in growth rates (Supplementary Table 1). Thus, we tested two faster growing derivatives of the slow-growing isolate P37005 that were obtained via passaging[77], as well as heterozygous and homozygous null mutants of the Clb4 mitotic cyclin that result in slower growth[78]. Each of these strains were compared on DDAs using fluconazole. We found no correlation between FoG and doubling time or between FoG and lag duration for either of the two lineages (Supplementary Fig. 5B). Thus, the two parameters that correlate with higher FoG values are (1) the proportion of cells that form colonies in the presence of drug (Fig. 3B), and (2) the more rapid appearance of colonies in the presence of drug, presumably reflecting shorter lag periods (Fig. 3E).

Taken together, these results indicate that two aspects of growth dynamics contribute to differences between low and high FoG isolates: high FoG strains have larger subpopulations that grow to form visible colonies at supra-MIC drug concentrations, and high FoG strains also form colonies more rapidly than strains with low FoG levels. This contrasts with tolerant bacterial cells with longer lag or quiescent periods that enable survival during bactericidal drug exposure. The distinctive growth properties of perseverant cells measured here as FoG/SMG in cells exposed to fungistatic drugs, and those measured for bacteria tolerant to cidal drugs indicate that mechanisms mediating drug responses are different in the two kingdoms. For

Figure 3

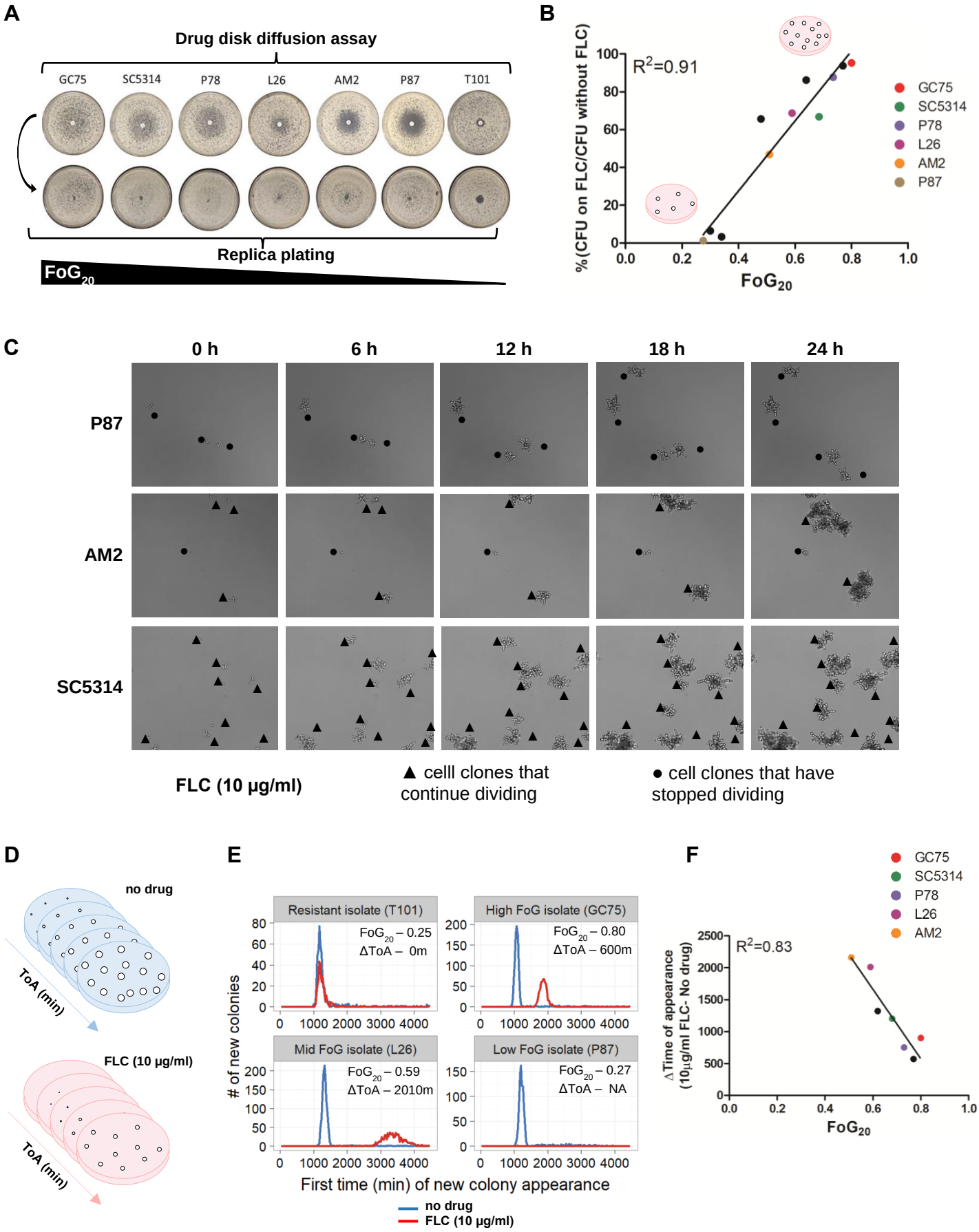
A
Drug disk diffusion assay
GC75
SC5314
P78
L26
AM2
P87
T101
Replica plating
FoG20
B
R2=0.91
%(CFU on FLC/CFU without FLC)
FoG20
GC75
SC5314
P78
L26
AM2
P87
C
0 h
6 h
12 h
18 h
24 h
P87
AM2
SC5314
FLC (10 µg/ml)
▲ celll clones that continue dividing
● cell clones that have stopped dividing
D
no drug
ToA (min)
FLC (10 µg/ml)
ToA (min)
E
Resistant isolate (T101)
FoG20 – 0.25
ΔToA – 0m
High FoG isolate (GC75)
FoG20 – 0.80
ΔToA – 600m
Mid FoG isolate (L26)
FoG20 – 0.59
ΔToA – 2010m
Low FoG isolate (P87)
FoG20 – 0.27
ΔToA – NA
# of new colonies
First time (min) of new colony appearance
no drug
FLC (10 µg/ml)
F
GC75
SC5314
P78
L26
AM2
R2=0.83
ΔTime of appearance (10µg/ml FLC- No drug)
FoG20

Figure 3. Growth analysis of cells growing within the ZOI (above MIC concentration). (a) Cells that grow within the ZOI are viable, as seen by replica plating of disk diffusion assays grown on casitone without fluconazole and incubated at 30°C for 48 h. (b) The degree of FoG for a given strain correlates with the proportion of colonies that are able to grow on 10 µg/ml fluconazole relative to growth on plates without fluconazole (n=11, P<0.001). (c) Microcolony analysis at supra-MIC concentrations of fluconazole (10 µg/ml). Black triangles indicate cells that continued dividing and black circles indicate cells that slowed or stopped dividing, respectively, over 24 h. Time lapse videos of these cells are available as Supplementary videos 1-3. FoG correlates with faster time of colony appearance. (d) Schematic of ScanLag analysis[75] that measures time of colony appearance (ToA), colony growth rate and colony size using desktop scanners. (e) Time of Appearance of colonies on medium without drug (blue) or with 10 µg/ml fluconazole (red) for resistant isolate T101, and isolates with different FoG levels. ~500 cells were plated per plates with or without 10 µg/ml fluconazole and scanned every 30 min for 96 h. Histograms show the number of colonies that appeared (y-axis) at each time point (x-axis). Data for additional isolates is presented in Supplementary Figure 4. (F) Correlation between FoG_{20} values and the difference (Δ) in the time of appearance of colonies in the presence vs absence of fluconazole (ΔToA = ToA with 10 µg/ml fluconazole – ToA without fluconazole). (n=7, *P*=0.0027)

example, tolerant bacterial cells do not grow within the ZOI of a DDA unless the drug disk is replaced with additional fresh medium[79], while perseverant cells, by definition, appear within the ZOI in DDAs even in the presence of drug. It is also likely that bacterial tolerance and fungal perseverance reflect different strategies of growth in cidal vs. static drugs. To highlight this distinction we chose a new term, *perseverance***,** to describe the ability of subpopulations of fungal cells to grow in the presence of supra-MIC drug concentrations.

Clinical persistence is associated with higher levels of perseverance

Fluconazole is often the first line of therapy for treating systemic *C. albicans* infections[80] and is also the major antifungal used in third world countries[81]. However, treatment with fluconazole often fails despite isolates being susceptible to the drug when tested *in vitro*. We obtained sets of clinical isolates that were either efficiently cleared by fluconazole treatment (non-persistent isolates) or that persisted in the host despite extended fluconazole therapy. Clinical persistence is defined here as two or more blood cultures positive for *C. albicans* on one or more days apart despite antifungal therapy. Non-persistent isolates (n = 7) were cleared from the bloodstream soon after fluconazole treatment was initiated. In contrast, persistent infections in 12 patients yielded serial isolates both prior to and throughout the course of treatment, with 3 to 9 isolates per patient (Fig. 4A and Supplementary Table 5). Clinical persistence in these patients occurred despite clinical MIC assays having established that all isolates were fluconazole susceptible, with MIC levels less than 1 µg/ml.

Each patient had a different clinical trajectory, all of them having central venous catheters that, in most cases, were removed upon detection of fungal infection. Importantly, none of the patients from which these isolates were collected were neutropenic or otherwise immunocompromised. All patients were treated with fluconazole as the first drug of choice and, in some cases, antifungal therapy was continued with either caspofungin or amphotericin B. Of

the 19 patients, 7 patients died during the 30 day follow up, 6 of which were unable to clear the fungal infection, although a causality between infection and death could not be determined.

We examined the drug responses of persistent and non-persistent isolates using DDAs and BMDAs as described above, and included three of the seven strains utilized above as additional controls (termed 'susceptible' isolates). As expected, persistent and non-persistent isolates displayed similar RAD and MIC levels of 0.25 to 1 µg/ml (Fig. 4B and Supplementary Fig. 6A-B), levels well below those of resistant strains (clinical MIC breakpoint = 4 µg/ml). The sole exception to this was the final isolate from series 3 (S03), which became fluconazole-resistant (MIC > 128 µg/ml) (R, Fig. 4C). For this series, the penultimate isolate, which had not acquired resistance (MIC = 0.5 µg/ml), was used in subsequent analyses. Strikingly, both FoG and SMG levels differed significantly between the two groups of clinical isolates (Fig. 4B,C): non-persistent isolates had average FoG values of 0.38 while persistent isolates had average FoG values almost 2-fold higher (0.59). For most of the series, FoG levels did not change significantly as the infection progressed, despite ongoing fluconazole therapy (Supplementary Fig. 6A). Similarly, SMG levels were an average of 1.4-fold higher in persistent than non-persistent isolates and this distinction in SMG levels between the two groups was clearly evident when SMG was measured at 48 h (Fig. 4C). By contrast, MIC levels did not change when analyzed at 24 h or 48 h (Supplementary Fig. 6B), reinforcing the idea that perseverance is time-dependent whereas susceptibility/resistance is not. SMG and FoG levels again correlated for both persistent and non-persistent isolates (Supplementary Fig. 6C), indicating that the two parameters measure features of the same phenomenon.

Taken together these results reveal that persistent isolates display significantly higher levels of growth at high drug concentrations compared to isolates that are clinically cleared by fluconazole treatment. In fact, many of the persistent isolates had FoG levels > 0.5, a level at which more than half of the cells in the population are able to grow, albeit more slowly, in the presence of antifungals (Fig. 3B). This is important because it indicates that perseverance is an

Figure 4

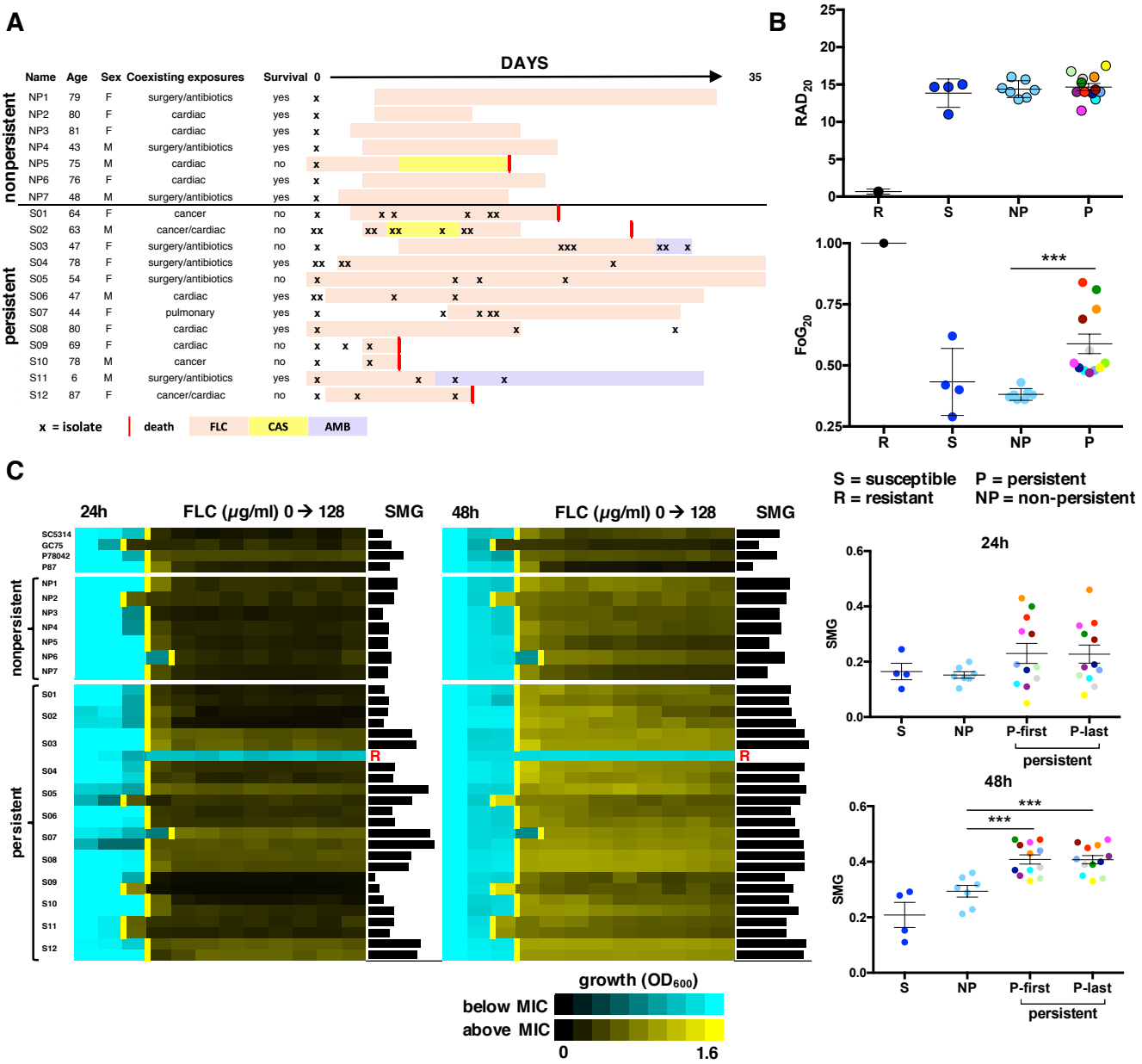

Figure 4. FoG and SMG levels differ between clinically persistent and non-persistent isolates. (a) Clinical history of 7 non-persistent isolates and 12 series of clinically persistent isolates showing the age, sex and associated conditions of the patients from whom they were isolated. 'X' symbols indicate the time when isolates were collected, shaded areas indicate the duration of antifungal therapy received (fluconazole, pink; caspofungin, yellow; amphotericin B, violet), red lines mark death events over a 30-day follow-up. (b) FoG and RAD levels for drug-susceptible (S, n = 4) isolates SC5314, GC75, P78042 and P87, resistant (R, n =1) isolate P60002[31], non-persistent isolates (NP, n = 7) and the first patient isolate from each of the series of clinically persistent

strains (P, n = 12). Asterisks indicate significant differences between persistent and non-persistent isolates (unpaired t-test, P = 0.67 for RAD, $P < 0.001$ for FoG). (c) Broth microdilution assays showing MIC and SMG levels at 24 and 48 h for the susceptible control strains (S, n = 4), the non-persistent isolates as in (b) (NP, n = 7) and for both the initial and final isolates for each of the 12 clinically persistent series (S01-12). The final isolate in S03 became fluconazole resistant (R), therefore the penultimate isolate in this series was included as well. Asterisks indicate significant differences between persistent and non-persistent isolates (unpaired t-test, NP vs P-first $P = 0.061$ and NP vs P-last $P = 0.053$ for SMG at 24 h, NP vs P-first $P < 0.001$ and NP vs P-last $P < 0.001$ for SMG at 48 h).

intrinsic property of clinical isolates distinct from drug resistance. Furthermore, perseverance contributes to the ability of an antifungal to clear an infection and thereby directly impacts clinical outcome.

Drug combinations primarily affect perseverance rather than resistance

Combination therapy is currently being explored as a strategy to extend the lifespan of available antifungal drugs[50,56,82,83]. We tested several adjuvant drugs reported to have additive or synergistic effects with fluconazole for their effects on FoG/SMG and RAD/MIC. These include aureobasidin A, an inhibitor of sphingolipid biosynthesis[46], rapamycin, an inhibitor of the mTOR signaling pathway[48,84], fluoxetine, a serotonin inhibitor reported to inhibit efflux pump activities[47], and fluphenazine, an antipsychotic drug that stimulates ABC transporter efflux pumps and indirectly inhibits calcineurin via calmodulin[49,85,86] (Fig. 5A). We found that none of these adjuvant drugs caused a significant change in susceptibility to fluconazole (i.e., there was no change in RAD), but all of them significantly reduced perseverance (FoG) to a baseline level. Adjuvant treatment led to clearing of FoG for all 7 strains tested, indicating that this is a common characteristic of diverse *C. albicans* isolates.

Inhibitors of Hsp90 (geldanamycin and radicicol), as well as inhibitors of calcineurin (cyclosporine A and FK506), yielded similar results in drug response assays. Thus, each of these compounds had no significant effect on RAD/MIC but significantly reduced both FoG and SMG to baseline levels (Fig. 5B and Supplementary Fig. 7A). Again, this was consistent across all isolates tested, including a series of clinical isolates from a single HIV patient [87,88] that had acquired increased MIC levels over time (Supplementary Fig. 7B,C). Similarly, for both the persistent and non-persistent clinical isolates FoG levels were reduced to baseline by the addition of adjuvant drugs including geldanamycin, rapamycin, FK506, fluphenazine and doxycycline (Supplementary Fig. 7D). As a consequence, FoG levels of persistent strains became indistinguishable from those of non-persistent strains. In contrast, and as seen with

Figure 5

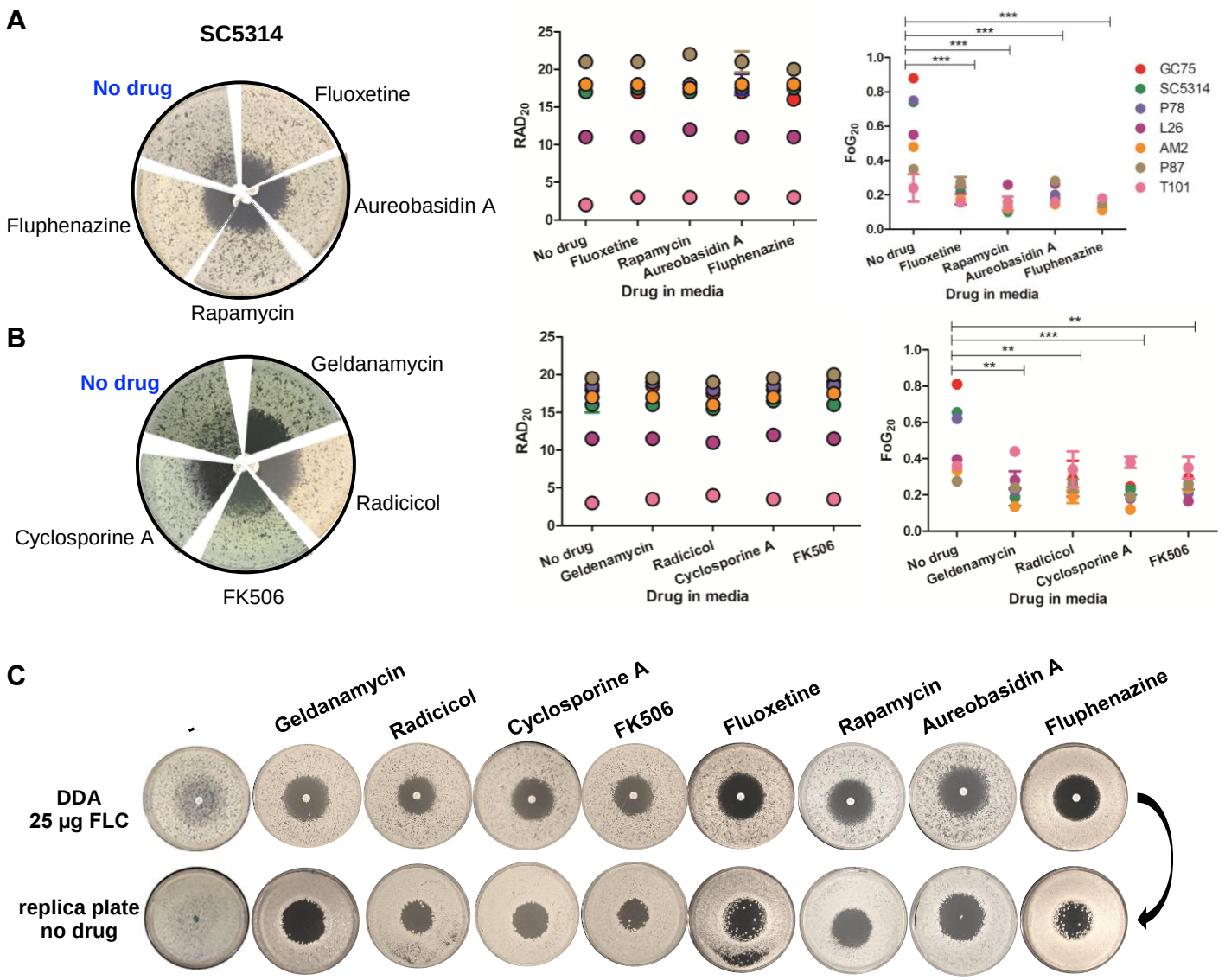

Figure 5. Adjuvant drugs significantly reduce fluconazole perseverance but not resistance and render fluconazole cidal rather than static. (a) Disk diffusion assays performed with 25 µg fluconazole disks on casitone plates supplemented with adjuvant drugs 20 µg/ml fluoxetine, 5 ng/ml aureobasidin A, 0.5 ng/ml rapamycin or 10 µg/ml fluphenazine for strain SC5314 (left), and RAD (middle panels) (1-way ANOVA, n groups=5 , P- 0.9998) and FoG (right panels) (1-way ANOVA, n groups=5 , P<0.0001) levels for strains as in Figure 1. (b) Disk diffusion assays as in (a) performed with casitone plates supplemented with Hsp90 inhibitors (0.5 µg/ml geldanamycin or 0.5 µg/ml radicicol) or calcineurin inhibitors (0.5 µg/ml FK506 or 0.4 µg/ml cyclosporine A) for strain SC5314 (left), and RAD (middle panels) (1-way ANOVA, n groups=5 , *P*- 0.9994) and FoG (right panels) (1-way ANOVA, n groups=5 , *P*=0.0004) levels. (c) Effect of drug adjuvants and inhibitors on the viability of cells growing inside the ZOI. Fluconazole disk diffusion assays from (a) and (b) were replica plated (after removal of the drug disk) onto casitone plates (without fluconazole or the adjuvant drugs/inhibitors) and incubated at 30°C for 48 h.

other isolates, RAD levels remained unchanged in response to most of these adjuvants (Supplementary Fig. 7D).

We conclude that exposure to inhibitors of either Hsp90 or calcineurin reduced growth within the ZOI (FoG) as well as growth above MIC levels in BMDAs (SMG). However, none of the inhibitors induced a significant change in MIC or RAD when measured at 24 h has recommended. Of note, geldanamycin (Supplementary Fig. 7E), as well as all the other adjuvant drugs, significantly reduced cell viability within the ZOI (Fig. 5C).

Genetic pathways affecting perseverance and/or resistance

We next explored whether genetic pathways that are known to contribute to drug responses affect perseverance. Toward this goal, we collected a series of mutant isolates, most of them constructed in various backgrounds of laboratory strain SC5314 (Supplementary Fig. 8A). As expected, most of the parental isolates exhibited similar RAD/MIC levels (Supplementary Table 2 and Supplementary Fig. 8B). Surprisingly, however, perseverance levels were significantly reduced in some of the parental control strains. Specifically, FoG levels dropped by ~40-50% in CAI-4 and many of its derivatives (Supplementary Table 2, Supplementary Fig. 8B and Supplementary Text 1). The inadvertent deletion of *IRO1* (because it is adjacent to *URA3)* is likely responsible for decreased perseverance levels in CAI-4 and many of its derivatives, as deletion of *IRO1* alone reduced FoG by ~42.5%. This implies that *IRO1,* which encodes a transcription factor involved in iron utilization[89], promotes higher FoG levels in *C. albicans* strains. Despite the effect of strain background differences, relative changes in FoG and RAD could be measured by comparing each mutant strain to the corresponding parental strain and, in some cases, to strains in which the deleted gene had been reintroduced (Supplementary Fig. 8B).

Given that calcineurin inhibitors reduced perseverance, we first tested null mutants lacking genes that encode the calcineurin subunits Cna1[68] and Cnb1[90], along with

independently constructed mutants lacking Crz1[91], the major transcription factor activated by calcineurin in response to drug stress. Null mutants in *CNA1, CNB1* and *CRZ1* constructed in two different parental strains (SC5314 and SN192) had significantly reduced perseverance (50-60%) yet displayed no significant change in RAD/MIC (Supplementary Table 3 and Fig. 6A). These results indicate that calcineurin promotes perseverance via the Crz1 transcription factor.

In contrast, deletion of genes encoding regulators of calcineurin, including *RCN1* and *RCN2,* had little effect on RAD or FoG when compared to isogenic parental strains (Supplementary Table 3 and Fig. 6A). Consistent with this, RAD and FoG levels in an *rcn1*ΔΔ/*crz1*ΔΔ mutant were similar to those of the *crz1*ΔΔ single mutants (Supplementary Table 3 and Fig. 6A). However, these data do not exclude the possibility that *RCN1* and *RCN2* could have functionally redundant roles in drug responses.

VPS21, a gene reported to affect 'tolerance' but not susceptibility or resistance to azoles was analyzed because estimates from published BMDA data indicated that *vps1*ΔΔ null mutants do not affect MIC at 24 h yet exhibit very high SMG at 48 h[10]**.** *VPS21* encodes a Rab GTPase that regulates endosomal trafficking through the late endosome. As expected, *vps21*ΔΔ null mutants did not alter RAD but displayed high FoG levels in DDAs relative to the parental strain (Supplementary Table 3 and Fig. 6A).

We also tested a strain lacking *CAS5* because of its reported role in fluconazole responses. *CAS5* encodes a transcription factor originally identified in *C. albicans* for its role in caspofungin survival[92] and was shown to enhance the cidality of fluconazole, especially when analyzed at 48 h rather than 24 h after drug exposure[93]. Indeed, the *cas5*ΔΔ mutant reduced FoG by 90% and increased RAD by 25% (Supplementary Table 3 and Fig. 6A), indicating that Cas5 affects perseverance dramatically and resistance more modestly.

We next analyzed the role of genes encoding transcription factors known to have roles in fluconazole resistance. These include Upc2, a transcription factor that regulates sterol uptake and ergosterol biosynthetic genes (ergosterol is the target of azoles[94]), Tac1 and Mrr1, which

Figure 6

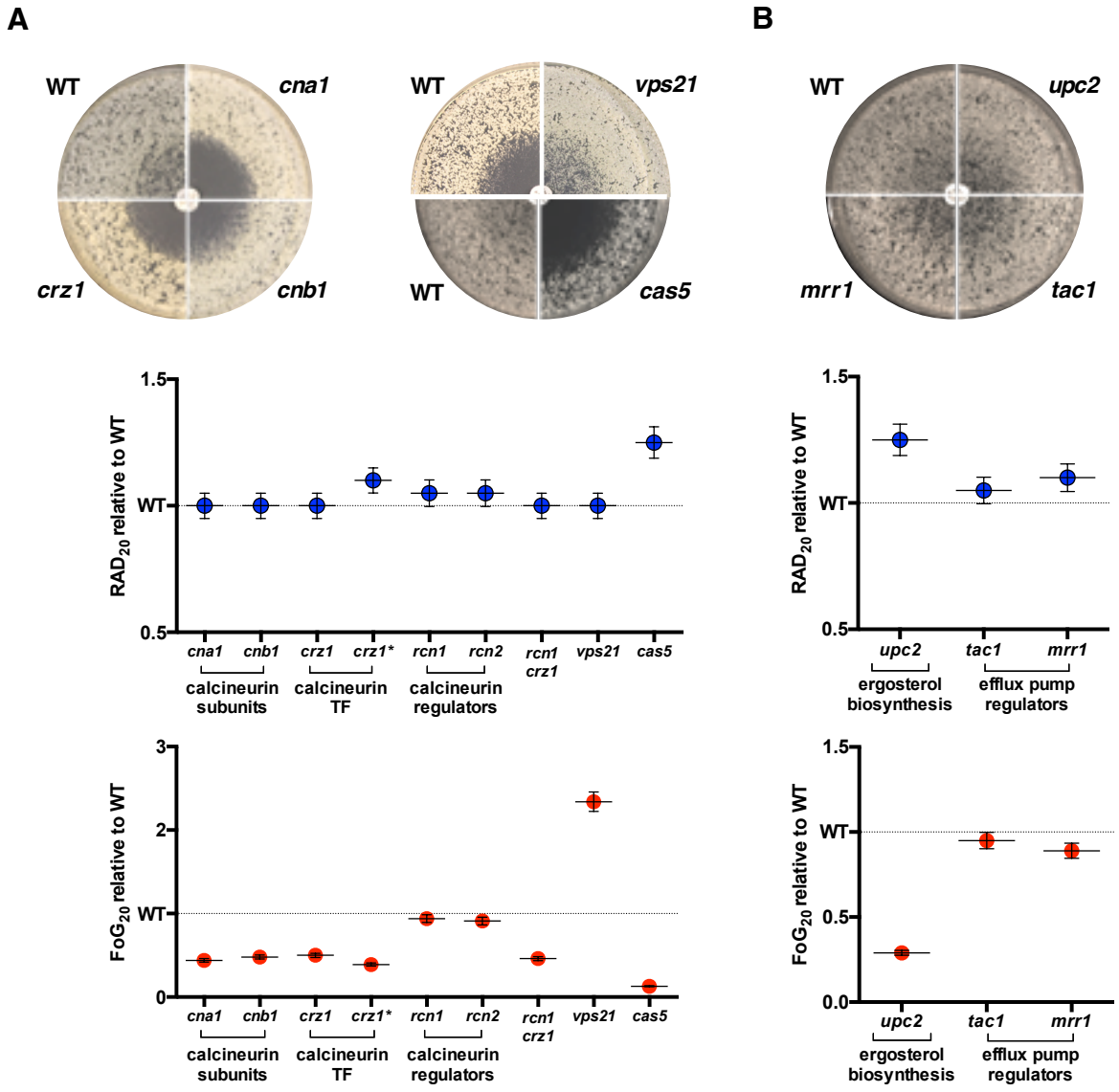

Figure 6. Effects of different pathways on perseverance and/or susceptibility to fluconazole. Disk diffusion assays performed using a series of mutants carrying deletions in (a) genes encoding calcineurin subunits Cna1 and Cna2, two separately constructed isolates lacking the calcineurin responsive transcription factor Crz1, a vacuolar trafficking protein Vps21, the Cas5 transcription factor up-regulated by fluconazole or (b) mutants lacking transcription factors known to regulate ergosterol gene expression (Upc2) or efflux pump expression (Tac1, Mrr1). Results for both *crz1* isolates were similar and only one is illustrated. These mutants as well as mutants lacking calcineurin regulators Rcn1 or Rcn2, and an *rcn1 crz1* double mutant were analyzed by *diskImageR,* and RAD and FoG levels, relative to the isogenic parental strain backgrounds are illustrated in the middle and lower rows, respectively. Pictures show representative images of two biological replicates (n = 2).

regulate the expression of ABC and MFS efflux genes, respectively. Like the *cas5*ΔΔ null mutant, *upc2*ΔΔ mutants affected both RAD (increased by 25%) and FoG (decreased by ~70%). In contrast, *tac1* and *mrr1* mutants had no significant effects on RAD or FoG (Supplementary Table 3 and Fig. 6B). This is consistent with the idea that there are multiple efflux pump genes and transcriptional regulators that control them, and that any one of them is likely to be redundant with efflux activity of the others sufficient for wild-type activity[95-97].

Together, these results show that different genetic pathways, such as calcineurin activity via Crz1, or that involving Iro1, contribute to increased perseverance levels while Vps21 and vacuolar membrane trafficking/homeostasis contribute to reduced perseverance levels. Other Transcription factors such as Cas5 or Upc2, affect both resistance and perseverance, either by independently regulating pathways in both processes or by additional mechanisms that remain to be discovered.

Discussion

Currently, decisions about therapeutic strategies to treat *Candida* infections are often based upon patient status, the infecting species and the level of resistance (MIC) to antifungal drugs. Here, we quantified and characterized a new drug response parameter termed *perseverance* that appears to be relevant for the persistence of *C. albicans* isolates in the clinic. Perseverance, measured as FoG or SMG, quantifies features previously described qualitatively as 'trailing growth'[10,11,25,26,67,69,98,99], 'tolerance'[12-16] or 'Hsp90-dependent resistance'[40,57,100-102]. Previous studies have suggested no strong correlation between these supra-MIC growth phenomena and virulence in either mouse models[17,18] or infection outcomes in the human host[20]. However, most of these studies analyzed immediate responses rather than clinical persistence or recurrence over longer time frames.

We show that perseverance is concentration-independent, is correlated with the size of the subpopulation that grows at drug concentrations above the MIC, and is inversely correlated

with the length of lag phase for these colonies. The mechanisms that determine the size of the subpopulation that can grow at supra-MIC concentrations remain to be determined. Importantly, we measure SMG and FoG relative to the MIC, utilizing standard assays measured on consecutive days, to provide information about both resistance and perseverance. We show that perseverance is influenced by pH, temperature, and nutritional inputs, as previously reported for trailing growth and tolerance[26,66,67,70]. The term "perseverance" was chosen as it describes the process rather than the assay, and it avoids confusion with tolerance mechanisms that promote survival in cidal drugs via longer lag phases[7,9]. While current descriptions of tolerance in bacteria have analyzed survival in cidal drugs, it remains possible that a growth strategy akin to fungal perseverance may be found in bacteria that divide in supra-MIC concentrations of bacteriostatic drugs.

Perseverance is dependent upon pathways that do not affect the MIC, and is sensitive to adjuvant drugs that not only reduce perseverance but also increase the cidality of fluconazole, which is generally fungistatic. This ability to 'clear the FoG' suggests that the adjuvant drugs must inactivate stress response pathways that are essential for perseverance and viability in the drug. The idea that Hsp90 and calcineurin affect drug responses in fungi is certainly not new, and the idea that they can affect the cidality of antifungals has also been reported[15,53,69,93,103-105]. However, this study clearly shows that these proteins, and the pathways they regulate, are important for a response to drug that is distinct from resistance and that specifically affects cell survival at supra-MIC antifungal concentrations.

Multiple pathways influence perseverance, some of which we identify in this study. Vps21, a protein involved in membrane trafficking, clearly impacts perseverance via its ability to increase cytoplasmic calcium stores[10,106], which, in turn, is likely to increase calcineurin activity. However, not all adjuvant drugs may act via the Hsp90/calcinuerin pathway. For example, it remains to be determined how the TOR pathway (inhibited by rapamycin), sphingolipid synthesis (inhibited by AbA), as well as the antidepressant fluoxetine and the antipsychotic

fluphenazine affect perseverance (Supplementary Tables 2 and 3). Interestingly, Pkc1 inhibitors phenocopy inhibitors of Hsp90 or calcineurin and render fluconazole cidal[101], suggesting that perseverance is likely to be mediated, at least in part, via the Pkc1 pathway. Furthermore, the effect of Pkc1 inhibitors on the clinical isolate series used in Supplementary Figure 5 was indistinguishable from the effect of geldanamycin on these isolates[101], thus we posit that Pkc1 is critical for perseverance but not for *bona fide* resistance. However, since genetic experiments found that *PKC1* is not required for calcineurin-dependent drug responses[101], the relationship between Pkc1 and perseverance is likely to require further study.

It is also unclear how *IRO1*, a gene that was inadvertently deleted in a commonly used *C. albicans* lineage, contributes to perseverance. One possibility is that it relates to the requirement for iron in the function of Erg11, which is a cytochrome p450 enzyme and the direct target of fluconazole. Of note, doxycycline reduces tolerance by chelating limited iron stores in the medium[15], and iron deprivation also regulates the expression of *HSP90* and *CRZ1* via calcineurin signaling[107]. Furthermore, the effect of doxycycline on iron availability is important to consider when studying azole responses using doxycycline to activate or repress the Tet promoter in engineered strains[108,109].

Similarly, we do not yet understand how transcription factors *CAS5* and *UPC2* affect both resistance and perseverance. One option is that they may regulate multiple independent pathways, some of which influence resistance and others that affect perseverance. A recent study supports this idea, given that *cas5*Δ/Δ strains cause altered promoter occupancy of RNA polymerase II at over 600 genes[110]. Alternatively, genes affecting resistance may also reduce the degree to which an antifungal drug causes cellular stress and thus may alter the requirement for the stress response mechanisms that drive perseverance.

Of more direct significance, this analysis of a well-matched set of clinically persistent and non-persistent isolates supports the hypothesis that strains with higher FoG/SMG levels may relate to the failure of antifungal drugs to clear an infection despite an isolate being drug

susceptible. The prolonged presence of isolates in the host could also contribute to the emergence of resistance by providing cells with a greater chance of acquiring mutations that render them drug resistant, a process that occurred in one of the patients with a persistent isolate. Measuring the perseverance level of an infecting isolate could facilitate useful clinical studies to determine the degree to which perseverance may predict which isolates are more likely to give rise to persistent and/or recurrent infections. In addition, we posit that quantifying perseverance may enable clinicians to determine when adding an adjuvant drug to increase the cidality of fluconazole would be most effective. This may be especially relevant when antifungals other than fluconazole are less accessible, for example in developing countries.

Methods

Strains. All strains (Supplementary Table 1) were streaked onto YPD plates and grown for 48 h at 30°C. A single colony from each strain was arbitrarily selected and frozen in 15% glycerol and stored at -80°C for all assays. For persistent and nonpersistent strains obtained from Brazilian patients, all ethical regulations were observed and the study was approved by the Ethical Committee of the Federal University of São Paulo (January, 2016, NO 9348151215).

Strain construction. To disrupt the two alleles of the *RCN2* gene we amplified (using primers BP1440 and BP1441, Supplementary Table 4) the flanking sequence of C7_01700W ORF using BJB-T 2 (*HIS1*) and BJB-T 61 (*ARG4*) plasmids as a template (Supplementary Table 4). Strain YJB-T65 was transformed with the PCR product to generate heterozygote mutant YJB-T 2214 (*rcn2::HIS1*) and subsequently homozygote mutant YJB-T2227 (*rcn2::HIS1 / rcn2::ARG4*). The disruptions were verified using primers BP1444 and BP1445.

Broth micro dilution assays. Minimal inhibitory concentration (MIC) for each strain was measured using CLSI M27-A2 guidelines[24] with minor modifications as follows. Strains were

512 streaked from frozen culture onto YPD agar and incubated for 24 h at 30°C. Colonies were
513 suspended in 1 ml PBS and diluted to 10^3 cells/ml in a 96 well plate with casitone containing a
514 gradient of two-fold dilutions per step of fluconazole, with the first well contain no drug. For
515 persistent and non-persistent clinical isolates, cells were grown overnight in YPD at 30°C and
516 diluted to 10^4 cells/ml in YPD containing a gradient of two-fold dilutions per step of fluconazole.
517 MIC_{50} levels were determined after 24 h or 48 h by taking an optical density reading (OD_{600})
518 after manual agitation of all wells on a Tecan plate reader (Infinite F200 PRO, Tecan,
519 Switzerland). MIC_{50} levels (shown as yellow lines on BMDA heatmaps) were determined as the
520 point at which the OD_{600} had been reduced by ≥50% compared to the no-drug wells.
521
522 **Disk diffusion assays.** The CLSI M44-A2 guidelines for antifungal disk diffusion susceptibility
523 testing[111] were followed with slight modifications. In brief, strains were streaked from frozen
524 culture onto YPD agar and incubated for 24 h at 30°C. Colonies were suspended in 1 ml PBS
525 and diluted to 1 x 10^6 cells/ml. 2 x 10^5 cells were spread onto 15 ml casitone (9 g/l Bacto
526 casitone, 5 g/l yeast extract, 15 g/l Bacto agar (BD Sparks, MD USA), 11.5 g/l sodium citrate
527 dehydrate and 2% glucose (Sigma-Aldrich, St. Louis, MO USA). For persistent and non-
528 persistent clinical isolates, cells were grown overnight in YPD and 10^5 cells were spread onto 15
529 ml YPD plates. To facilitate comparisons between casitone and YPD disk diffusion assays, a
530 subset of control strains with diverse FoG levels were included in both types of assays
531 (SC5314, GC75, P87). For disk assays with drug adjuvants, the following concentrations of
532 drugs were used: 0.5 µg/ml geldanamycin, 0.5 µg/ml radicicol, 0.5 µg/ml FK506, 0.4 µg/ml
533 cyclosporine A, 20 µg/ml fluoxetine, 5 ng/ml aureobasidin A, 0.5 ng/ml rapamycin, 10 µg/ml
534 fluphenazine and 50 µg/ml doxycycline. A single 25 µg fluconazole disk (6 mm, Oxoid, UK or
535 Liofilchem, Italy) was placed in the center of each plate, plates were then incubated at 30°C for
536 48 h, and each plate was photographed individually. Analysis of the disk diffusion assay was
537 done using the *diskImageR* pipeline[66] and the R script is available at

https://github.com/acgerstein/diskImageR/tree/master/inst .

ScanLag assay. The ScanLag assay was adapted from[75] with minor modifications. Strains were streaked from frozen culture onto YPD agar and incubated for 24 h at 30°C. Colonies were suspended in 1 ml PBS, diluted to 10^4 cell/ml and 2 x 10^3 cells (200 µl) were spread onto 15 ml casitone plates with or without 10 µg/ml fluconazole (DMSO, Ofer Chemical Laboratory, Israel). Plates were placed on the scanners at 30°C and scanned every 30 min for 72 h. Analysis of the images was done in MATLAB using the "ScanLag" script[75] that was adjusted to yeast cells by changing the identification of the size of the colony to a minimum of 20 pixels.

Viability assays. Replica plating was performed from disk diffusion plates that were incubated at 30°C for 48 h. Master plates were inverted and pressed firmly on a sterile cotton velveteen stamp and then transferred to new casitone plates containing no drug. Replica plates were incubated at 30°C for 48 h, and then each plate was photographed individually.

Growth assays. To determine growth parameters (doubling time and lag phase duration), *C. albicans* cells were seeded at a concentration of 2 x 10^5 cells/ml in 96-well plates containing YPD media. Plates were grown for 48 h at 30°C with continuous shaking in a Tecan plate reader and the optical density reading (OD_{600}) of all wells was recorded every 15 min. Measurements of doubling time and lag phase duration were obtained from 3 biological replicates, each performed in duplicate.

Microcolony assays. Microcolony assays were adapted from[74] with minor modifications. Colonies were suspended in 3 ml casitone media and grown overnight in 30°C. Cultures were

diluted 1:30 in casitone and incubated at 30°C until cultures reached logarithmic phase (~3-4 h) and diluted to 10^4 cells/ml in casitone.

Microscopy. Glass-bottomed 24-well plates (De-GROOT, Israel) were coated with 1 ml of a 200 µg/ml Concanvalin A solution (Type VI, Sigma-Aldrich, St. Louis, MO USA) for 3-4 h. Wells were washed twice with 1 ml ddH20 and 10^4 cells/ml in a 2 ml volume were added to wells with or without 10 µg/ml fluconazole. Plates were sealed with an optically clear film (Axygen breathing sealing film, Corning, Israel) and spun at 1200 rpm for 1 min. Images where captured in 100 fields per well for 48 h in 1 h intervals using a Nikon Ti Eclipse microscope equipped with a full-stage environmental chamber (set to 30°C) with a Nikon Plan Apo 10x (0.45 numerical aperture) objective using Nikon Elements AR software. Focus coordinates and the positions over the plate surface was assigned using homemade R-and C-based scripts (adapted from[74] by Dr. Naomi Ziv). Automated Image analysis, including image processing and microscope control routines were written in Matlab, R, C, and shell scripts were adapted from [74].

Statistical analyses. All experiments represent the average of three or more biological repeats, with two technical repeats of each. Error bars represent the standard deviation. Statistics were performed using Microsoft Excel 2016 (Microsoft Corporation) and Prism 6 (GraphPad). The statistical tests performed were two-tailed Student's t tests, one way ANOVAs for comparisons between groups, and Tukey's multiple comparison tests. R squared tests were used for linear regressions. Significance was assigned for *P* values smaller than 0.05, asterisks denote P values as follows: ***, $P < 0.001$; **, $P < 0.01$; *, $P < 0.05$.

Data availability. The authors declare that all data supporting the findings of the study are available in this article and its Supplementary Information files, or from the corresponding author upon request.

Acknowledgements

We thank members of the Berman and Bennett labs for stimulating discussions throughout the work. G. Palmer, M. Lohse, O. Homann, A. Johnson, R. Ben-Ami, T. White, D. Soll, D. McCallum, F. Odds, D. Sanglard, L. Cowen, P.T. Magee, B. Cormack, P. Magwene, M. Kupiec, W. Fonzi, S. Noble, B.M. Vincent, S. Lindquist, and A. Colombo for providing strains and Naomi Ziv, Naama Droor and Stephanie Diezmann for helpful comments on the manuscript.

This work was funded by European Research Council Advanced Award 340087 (RAPLODAPT) to JB, by Fundação de Amparo a Pesquisa do Estado de São Paulo (FAPESP), Brazil to ALC, by National Institutes of Health grant AI081704 to RJB and by a Brazil Initiative Collaborative Grant from the Watson Institute to RJB and IVE.

Author contributions

IVE, RJB and JB designed the study; AR, IVE and AD collected the data; AR and IVE analyzed the data, ESS constructed mutant isolates, ALC provided clinical isolates and clinical input to the paper; AR, IVE, RJB and JB wrote the manuscript.

References

1. Pfaller, M.A. & Diekema, D.J. Progress in antifungal susceptibility testing of *Candida* spp. by use of Clinical and Laboratory Standards Institute broth microdilution methods, 2010 to 2012. *J Clin Microbiol* **50**, 2846-56 (2012).
2. Rex, J.H. & Pfaller, M.A. Has antifungal susceptibility testing come of age? *Clin Infect Dis* **35**, 982-9 (2002).
3. Pfaller, M.A. *et al.* Wild-type MIC distributions and epidemiological cutoff values for amphotericin B, flucytosine, and itraconazole and *Candida* spp. as determined by CLSI broth microdilution. *J Clin Microbiol* **50**, 2040-6 (2012).
4. Alexander, B.D. *et al.* Increasing echinocandin resistance in *Candida glabrata*: clinical failure correlates with presence of *FKS* mutations and elevated minimum inhibitory concentrations. *Clin Infect Dis* **56**, 1724-32 (2013).
5. Doern, G.V. & Brecher, S.M. The Clinical Predictive Value (or Lack Thereof) of the Results of *In Vitro* Antimicrobial Susceptibility Tests. *Journal of Clinical Microbiology* **49**(2011).
6. Vogwill, T., Comfort, A.C., Furio, V. & MacLean, R.C. Persistence and resistance as complementary bacterial adaptations to antibiotics. *J Evol Biol* **29**, 1223-33 (2016).
7. Brauner, A., Fridman, O., Gefen, O. & Balaban, N.Q. Distinguishing between resistance, tolerance and persistence to antibiotic treatment. *Nat Rev Microbiol* **14**, 320-30 (2016).
8. Balaban, N.Q., Merrin, J., Chait, R., Kowalik, L. & Leibler, S. Bacterial persistence as a phenotypic switch. *Science* **305**, 1622-5 (2004).
9. Fridman, O., Goldberg, A., Ronin, I., Shoresh, N. & Balaban, N.Q. Optimization of lag time underlies antibiotic tolerance in evolved bacterial populations. *Nature* **513**, 418-21 (2014).

10. Luna-Tapia, A., Kerns, M.E., Eberle, K.E., Jursic, B.S. & Palmer, G.E. Trafficking through the late endosome significantly impacts *Candida albicans* tolerance of the azole antifungals. *Antimicrob Agents Chemother* **59**, 2410-20 (2015).

11. Whaley, S.G. *et al.* The *RTA3* Gene, Encoding a Putative Lipid Translocase, Influences the Susceptibility of *Candida albicans* to Fluconazole. *Antimicrob Agents Chemother* **60**, 6060-6 (2016).

12. Tscherner, M. *et al.* The *Candida albicans* Histone Acetyltransferase Hat1 Regulates Stress Resistance and Virulence via Distinct Chromatin Assembly Pathways. *PLoS Pathog* **11**, e1005218 (2015).

13. Xu, D., Cheng, J., Cao, C., Wang, L. & Jiang, L. Genetic interactions between Rch1 and the high-affinity calcium influx system Cch1/Mid1/Ecm7 in the regulation of calcium homeostasis, drug tolerance, hyphal development and virulence in *Candida albicans*. *FEMS Yeast Res* **15**(2015).

14. Nagao, J. *et al.* Candida albicans Msi3p, a homolog of the *Saccharomyces cerevisiae* Sse1p of the Hsp70 family, is involved in cell growth and fluconazole tolerance. *FEMS Yeast Res* **12**, 728-37 (2012).

15. Fiori, A. & Van Dijck, P. Potent synergistic effect of doxycycline with fluconazole against *Candida albicans* is mediated by interference with iron homeostasis. *Antimicrob Agents Chemother* **56**, 3785-96 (2012).

16. Delarze, E. & Sanglard, D. Defining the frontiers between antifungal resistance, tolerance and the concept of persistence. *Drug Resist Updat* **23**, 12-19 (2015).

17. Rex, J.H. *et al.* Optimizing the correlation between results of testing *in vitro* and therapeutic outcome *in vivo* for fluconazole by testing critical isolates in a murine model of invasive candidiasis. *Antimicrob Agents Chemother* **42**, 129-34 (1998).

18. Arthington-Skaggs, B.A., Warnock, D.W. & Morrison, C.J. Quantitation of *Candida albicans* ergosterol content improves the correlation between *in vitro* antifungal

susceptibility test results and *in vivo* outcome after fluconazole treatment in a murine model of invasive candidiasis. *Antimicrob Agents Chemother* **44**, 2081-5 (2000).

19. Peters, B.M. *et al.* An Azole-Tolerant Endosomal Trafficking Mutant of *Candida albicans* Is Susceptible to Azole Treatment in a Mouse Model of Vaginal Candidiasis. *Antimicrob Agents Chemother* **61**(2017).

20. Revankar, S.G. *et al.* Interpretation of trailing endpoints in antifungal susceptibility testing by the National Committee for Clinical Laboratory Standards method. *J Clin Microbiol* **36**, 153-6 (1998).

21. Rueda, C. *et al.* Evaluation of the possible influence of trailing and paradoxical effects on the clinical outcome of patients with candidemia. *Clin Microbiol Infect* **23**, 49 e1-49 e8 (2017).

22. Chang, T.P. *et al.* Distribution and drug susceptibilities of *Candida* species causing candidemia from a medical center in central Taiwan. *J Infect Chemother* **19**, 1065-71 (2013).

23. Marcos-Zambrano, L.J., Escribano, P., Sanchez-Carrillo, C., Bouza, E. & Guinea, J. Scope and frequency of fluconazole trailing assessed using EUCAST in invasive *Candida* spp. isolates. *Med Mycol* **54**, 733-9 (2016).

24. CLSI. Reference method for broth dilution antifungal susceptibility testing of yeasts; 4th Informational Supplement. *CLSI document M27-S4. Wayne: Clinical and Laboratory Standards Institute; .* (2012).

25. Coenye, T., De Vos, M., Vandenbosch, D. & Nelis, H. Factors influencing the trailing endpoint observed in *Candida albicans* susceptibility testing using the CLSI procedure. *Clin Microbiol Infect* **14**, 495-7 (2008).

26. Agrawal, D., Patterson, T.F., Rinaldi, M.G. & Revankar, S.G. Trailing end-point phenotype of *Candida* spp. in antifungal susceptibility testing to fluconazole is eliminated by altering incubation temperature. *J Med Microbiol* **56**, 1003-4 (2007).

27. Arendrup, M.C., Cuenca-Estrella, M., Lass-Florl, C. & Hope, W. EUCAST technical note on the EUCAST definitive document EDef 7.2: method for the determination of broth dilution minimum inhibitory concentrations of antifungal agents for yeasts EDef 7.2 (EUCAST-AFST). *Clin Microbiol Infect* **18**, E246-7 (2012).

28. Forche, A. *et al.* The parasexual cycle in *Candida albicans* provides an alternative pathway to meiosis for the formation of recombinant strains. *PLoS Biol* **6**, e110 (2008).

29. Harrison, B.D. *et al.* A tetraploid intermediate precedes aneuploid formation in yeasts exposed to fluconazole. *PLoS Biol* **12**, e1001815 (2014).

30. Bennett, R.J. & Johnson, A.D. Completion of a parasexual cycle in *Candida albicans* by induced chromosome loss in tetraploid strains. *The EMBO journal* **22**, 2505-2515 (2003).

31. Hirakawa, M.P. *et al.* Genetic and phenotypic intra-species variation in *Candida albicans. Genome Res* **25**, 413-25 (2015).

32. Feri, A. *et al.* Analysis of Repair Mechanisms following an Induced Double-Strand Break Uncovers Recessive Deleterious Alleles in the *Candida albicans* Diploid Genome. *MBio* **7**(2016).

33. Ford, C.B. *et al.* The evolution of drug resistance in clinical isolates of *Candida albicans*. *Elife* **4**, e00662 (2015).

34. Muzzey, D., Schwartz, K., Weissman, J.S. & Sherlock, G. Assembly of a phased diploid *Candida albicans* genome facilitates allele-specific measurements and provides a simple model for repeat and indel structure. *Genome Biol* **14**, R97 (2013).

35. Tavanti, A., Gow, N.A., Senesi, S., Maiden, M.C. & Odds, F.C. Optimization and validation of multilocus sequence typing for *Candida albicans*. *J Clin Microbiol* **41**, 3765-76 (2003).

36. MacCallum, D.M. *et al.* Property differences among the four major *Candida albicans* strain clades. *Eukaryot Cell* **8**, 373-87 (2009).

37. McManus, B.A. & Coleman, D.C. Molecular epidemiology, phylogeny and evolution of *Candida albicans*. *Infect Genet Evol* **21**, 166-78 (2014).

38. Odds, F.C. In *Candida albicans*, resistance to flucytosine and terbinafine is linked to *MAT* locus homozygosity and multilocus sequence typing clade 1. *FEMS Yeast Res* **9**, 1091-101 (2009).

39. Whaley, S.G. *et al.* Azole Antifungal Resistance in *Candida albicans* and Emerging Non-albicans *Candida* Species. *Front Microbiol* **7**, 2173 (2016).

40. Cowen, L.E., Carpenter, A.E., Matangkasombut, O., Fink, G.R. & Lindquist, S. Genetic architecture of Hsp90-dependent drug resistance. *Eukaryot Cell* **5**, 2184-8 (2006).

41. Youngsaye, W. *et al.* Overcoming fluconazole resistance in *Candida albicans* clinical isolates with tetracyclic indoles. *Bioorg Med Chem Lett* **22**, 3362-5 (2012).

42. Taipale, M., Jarosz, D.F. & Lindquist, S. *HSP90* at the hub of protein homeostasis: emerging mechanistic insights. *Nature Reviews Molecular Cell Biology* **11**, 515-528 (2010).

43. Pratt, W.B. & Toft, D.O. Regulation of signaling protein function and trafficking by the hsp90/hsp70-based chaperone machinery. *Exp Biol Med (Maywood)* **228**, 111-33 (2003).

44. Cowen, L.E. & Steinbach, W.J. Stress, drugs, and evolution: the role of cellular signaling in fungal drug resistance. *Eukaryot Cell* **7**, 747-64 (2008).

45. Khalili, V., Shokri, H., Khosravi, A.R., Akim, A. & Amri Saroukolaei, S. Purification and comparison of heat shock protein 90 (Hsp90) in *Candida albicans* isolates from Malaysian and Iranian patients and infected mice. *J Mycol Med* **26**, 94-102 (2016).

46. Zhong, W., Jeffries, M.W. & Georgopapadakou, N.H. Inhibition of inositol phosphorylceramide synthase by aureobasidin A in *Candida* and *Aspergillus* species. *Antimicrob Agents Chemother* **44**, 651-3 (2000).

47. Gu, W., Guo, D., Zhang, L., Xu, D. & Sun, S. The Synergistic Effect of Azoles and Fluoxetine against Resistant *Candida albicans* Strains Is Attributed to Attenuating Fungal Virulence. *Antimicrob Agents Chemother* **60**, 6179-88 (2016).

48. Cruz, M.C. *et al.* Rapamycin and less immunosuppressive analogs are toxic to *Candida albicans* and *Cryptococcus neoformans* via FKBP12-dependent inhibition of TOR. *Antimicrob Agents Chemother* **45**, 3162-70 (2001).

49. Henry, K.W., Cruz, M.C., Katiyar, S.K. & Edlind, T.D. Antagonism of azole activity against *Candida albicans* following induction of multidrug resistance genes by selected antimicrobial agents. *Antimicrob Agents Chemother* **43**, 1968-74 (1999).

50. Robbins, N., Wright, G.D. & Cowen, L.E. Antifungal Drugs: The Current Armamentarium and Development of New Agents. *Microbiol Spectr* **4**(2016).

51. Robbins, N. *et al.* An Antifungal Combination Matrix Identifies a Rich Pool of Adjuvant Molecules that Enhance Drug Activity against Diverse Fungal Pathogens. *Cell Rep* **13**, 1481-92 (2015).

52. Liu, S. *et al.* Combination of fluconazole with non-antifungal agents: a promising approach to cope with resistant *Candida albicans* infections and insight into new antifungal agent discovery. *Int J Antimicrob Agents* **43**, 395-402 (2014).

53. Uppuluri, P., Nett, J., Heitman, J. & Andes, D. Synergistic effect of calcineurin inhibitors and fluconazole against *Candida albicans* biofilms. *Antimicrob Agents Chemother* **52**, 1127-32 (2008).

54. Cowen, L.E. *et al.* Harnessing Hsp90 function as a powerful, broadly effective therapeutic strategy for fungal infectious disease. *Proc Natl Acad Sci U S A* **106**, 2818-23 (2009).

55. Cowen, L.E., Sanglard, D., Howard, S.J., Rogers, P.D. & Perlin, D.S. Mechanisms of Antifungal Drug Resistance. *Cold Spring Harbor Perspectives in Medicine* **5**(2015).

56. Veri, A. & Cowen, L.E. Progress and prospects for targeting Hsp90 to treat fungal infections. *Parasitology* **141**, 1127-1137 (2014).

57. Cowen, L.E. & Lindquist, S. Hsp90 potentiates the rapid evolution of new traits: drug resistance in diverse fungi. *Science* **309**, 2185-9 (2005).

58. Cowen, L.E. The evolution of fungal drug resistance: modulating the trajectory from genotype to phenotype. *Nat Rev Microbiol* **6**, 187-98 (2008).

59. Vogelaar, I.P. *et al.* Recurrent candidiasis and early-onset gastric cancer in a patient with a genetically defined partial *MYD88* defect. *Fam Cancer* **15**, 289-96 (2016).

60. Alves de Medeiros, A.K. *et al.* Chronic and Invasive Fungal Infections in a Family with CARD9 Deficiency. *J Clin Immunol* **36**, 204-9 (2016).

61. Ferwerda, B. *et al.* Human dectin-1 deficiency and mucocutaneous fungal infections. *The New England journal of medicine* **361**, 1760-1767 (2009).

62. Da Matta, D.A. *et al.* Multilocus sequence typing of sequential *Candida albicans* isolates from patients with persistent or recurrent fungemia. *Med Mycol* **48**, 757-62 (2010).

63. Pfaller, M.A. & Diekema, D.J. Epidemiology of invasive candidiasis: a persistent public health problem. *Clinical microbiology reviews* **20**, 133-163 (2007).

64. Chapman, R.L. & Faix, R.G. Persistently positive cultures and outcome in invasive neonatal candidiasis. *Pediatr Infect Dis J* **19**, 822-7 (2000).

65. Hammoud, M.S., Al-Taiar, A., Fouad, M., Raina, A. & Khan, Z. Persistent candidemia in neonatal care units: risk factors and clinical significance. *Int J Infect Dis* **17**, e624-8 (2013).

66. Gerstein, A.C., Rosenberg, A., Hecht, I. & Berman, J. diskImageR: quantification of resistance and tolerance to antimicrobial drugs using disk diffusion assays. *Microbiology* **162**, 1059-68 (2016).

67. Marr, K.A., Rustad, T.R., Rex, J.H. & White, T.C. The trailing end point phenotype in antifungal susceptibility testing is pH dependent. *Antimicrob Agents Chemother* **43**, 1383-6 (1999).

68. Sanglard, D., Ischer, F., Marchetti, O., Entenza, J. & Bille, J. Calcineurin A of *Candida albicans*: involvement in antifungal tolerance, cell morphogenesis and virulence. *Mol Microbiol* **48**, 959-76 (2003).

69. Marchetti, O., Moreillon, P., Glauser, M.P., Bille, J. & Sanglard, D. Potent synergism of the combination of fluconazole and cyclosporine in *Candida albicans*. *Antimicrob Agents Chemother* **44**, 2373-81 (2000).

70. Alp, S., Sancak, B., Hascelik, G. & Arikan, S. Influence of different susceptibility testing methods and media on determination of the relevant fluconazole minimum inhibitory concentrations for heavy trailing *Candida* isolates with low-high phenotype. *Mycoses* **53**, 475-80 (2010).

71. Oxman, D.A. *et al.* Candidaemia associated with decreased *in vitro* fluconazole susceptibility: is *Candida* speciation predictive of the susceptibility pattern? *J Antimicrob Chemother* **65**, 1460-5 (2010).

72. Pfaller, M.A., Jones, R.N. & Castanheira, M. Regional data analysis of *Candida non-albicans* strains collected in United States medical sites over a 6-year period, 2006-2011. *Mycoses* **57**, 602-11 (2014).

73. Pfaller, M.A., Messer, S.A., Moet, G.J., Jones, R.N. & Castanheira, M. *Candida* bloodstream infections: comparison of species distribution and resistance to echinocandin and azole antifungal agents in Intensive Care Unit (ICU) and non-ICU settings in the SENTRY Antimicrobial Surveillance Program (2008-2009). *International journal of antimicrobial agents* **38**, 65-69 (2011).

74. Levy, S.F., Ziv, N. & Siegal, M.L. Bet hedging in yeast by heterogeneous, age-correlated expression of a stress protectant. *PLoS Biol* **10**, e1001325 (2012).

75. Levin-Reisman, I., Fridman, O. & Balaban, N.Q. ScanLag: high-throughput quantification of colony growth and lag time. *J Vis Exp* (2014).

76. Levin-Reisman, I. *et al.* Automated imaging with ScanLag reveals previously undetectable bacterial growth phenotypes. *Nat Methods* **7**, 737-9 (2010).

77. Alby, K. & Bennett, R.J. Stress-induced phenotypic switching in *Candida albicans*. *Molecular biology of the cell* **20**, 3178-3191 (2009).

78. Bensen, E.S., Clemente-Blanco, A., Finley, K.R., Correa-Bordes, J. & Berman, J. The mitotic cyclins Clb2p and Clb4p affect morphogenesis in *Candida albicans*. *Mol Biol Cell* **16**, 3387-400 (2005).

79. Gefen, O., Chekol, B., Strahilevitz, J. & Balaban, N.Q. TDtest: easy detection of bacterial tolerance and persistence in clinical isolates by a modified disk-diffusion assay. *Sci Rep* **7**, 41284 (2017).

80. Spellberg, B.J., Filler, S.G. & Edwards, J.E., Jr. Current treatment strategies for disseminated candidiasis. *Clinical infectious diseases : an official publication of the Infectious Diseases Society of America* **42**, 244-251 (2006).

81. Jadhav, M.P. & Kshirsagar, N.A. Access to antifungal medicines in resource-poor countries. *Lancet Infect Dis* **14**, 370-1 (2014).

82. Shrestha, S.K., Fosso, M.Y. & Garneau-Tsodikova, S. A combination approach to treating fungal infections. *Sci Rep* **5**, 17070 (2015).

83. Chaturvedi, V. *et al.* Multilaboratory testing of two-drug combinations of antifungals against *Candida albicans*, *Candida glabrata*, and *Candida parapsilosis*. *Antimicrob Agents Chemother* **55**, 1543-8 (2011).

84. Chen, S.C., Lewis, R.E. & Kontoyiannis, D.P. Direct effects of non-antifungal agents used in cancer chemotherapy and organ transplantation on the development and virulence of *Candida* and *Aspergillus* species. *Virulence* **2**, 280-95 (2011).

85. Cyert, M.S. Genetic analysis of calmodulin and its targets in *Saccharomyces cerevisiae*. *Annu Rev Genet* **35**, 647-72 (2001).

86. Sanglard, D., Ischer, F., Marchetti, O., Entenza, J. & Bille, J. Calcineurin A of *Candida albicans*: involvement in antifungal tolerance, cell morphogenesis and virulence. *Molecular microbiology* **48**, 959-976 (2003).

87. White, T.C. Increased mRNA levels of *ERG16*, *CDR*, and *MDR1* correlate with increases in azole resistance in *Candida albicans* isolates from a patient infected with human immunodeficiency virus. *Antimicrob Agents Chemother* **41**, 1482-7 (1997).

88. Redding, S. *et al.* Resistance of *Candida albicans* to fluconazole during treatment of oropharyngeal candidiasis in a patient with AIDS: documentation by *in vitro* susceptibility testing and DNA subtype analysis. *Clin Infect Dis* **18**, 240-2 (1994).

89. Garcia, M.G. *et al.* Isolation of a *Candida albicans* gene, tightly linked to *URA3*, coding for a putative transcription factor that suppresses a *Saccharomyces cerevisiae aft1* mutation. *Yeast* **18**, 301-11 (2001).

90. Vincent, B.M., Lancaster, A.K., Scherz-Shouval, R., Whitesell, L. & Lindquist, S. Fitness trade-offs restrict the evolution of resistance to amphotericin B. *PLoS Biol* **11**, e1001692 (2013).

91. Karababa, M. *et al. CRZ1*, a target of the calcineurin pathway in *Candida albicans*. *Mol Microbiol* **59**, 1429-51 (2006).

92. Bruno, V.M. *et al.* Control of the *C. albicans* cell wall damage response by transcriptional regulator Cas5. *PLoS Pathog* **2**, e21 (2006).

93. Vasicek, E.M. *et al.* Disruption of the transcriptional regulator Cas5 results in enhanced killing of *Candida albicans* by Fluconazole. *Antimicrob Agents Chemother* **58**, 6807-18 (2014).

94. Vasicek, E.M., Berkow, E.L., Flowers, S.A., Barker, K.S. & Rogers, P.D. *UPC2* is universally essential for azole antifungal resistance in *Candida albicans*. *Eukaryot Cell* **13**, 933-46 (2014).

95. Pfaller, M.A. Antifungal drug resistance: mechanisms, epidemiology, and consequences for treatment. *Am J Med* **125**, S3-13 (2012).

96. Prasad, R., Gaur, N.A., Gaur, M. & Komath, S.S. Efflux pumps in drug resistance of *Candida*. *Infect Disord Drug Targets* **6**, 69-83 (2006).

97. Schubert, S. *et al.* Regulation of efflux pump expression and drug resistance by the transcription factors Mrr1, Upc2, and Cap1 in *Candida albicans*. *Antimicrob Agents Chemother* **55**, 2212-23 (2011).

98. Zomorodian, K. *et al. In Vitro* Susceptibility and Trailing Growth Effect of Clinical Isolates of *Candida* Species to Azole Drugs. *Jundishapur J Microbiol* **9**, e28666 (2016).

99. Braga-Silva, L.A. *et al.* Trailing end-point phenotype antibiotic-sensitive strains of *Candida albicans* produce different amounts of aspartyl peptidases. *Braz J Med Biol Res* **42**, 765-70 (2009).

100. Shapiro, R.S., Zaas, A.K., Betancourt-Quiroz, M., Perfect, J.R. & Cowen, L.E. The Hsp90 co-chaperone Sgt1 governs *Candida* albicans morphogenesis and drug resistance. *PLoS One* **7**, e44734 (2012).

101. LaFayette, S.L. *et al.* PKC signaling regulates drug resistance of the fungal pathogen *Candida albicans* via circuitry comprised of Mkc1, calcineurin, and Hsp90. *PLoS Pathog* **6**, e1001069 (2010).

102. Singh, S.D. *et al.* Hsp90 governs echinocandin resistance in the pathogenic yeast *Candida albicans* via calcineurin. *PLoS Pathog* **5**, e1000532 (2009).

103. Liu, S. *et al.* Synergistic Effect of Fluconazole and Calcium Channel Blockers against Resistant *Candida albicans*. *PLoS One* **11**, e0150859 (2016).

104. Onyewu, C., Blankenship, J.R., Del Poeta, M. & Heitman, J. Ergosterol biosynthesis inhibitors become fungicidal when combined with calcineurin inhibitors against *Candida albicans*, *Candida glabrata*, and *Candida krusei*. *Antimicrob Agents Chemother* **47**, 956-64 (2003).

105. Epp, E. *et al.* Reverse genetics in *Candida albicans* predicts ARF cycling is essential for drug resistance and virulence. *PLoS Pathog* **6**, e1000753 (2010).

106. Luna-Tapia, A., Tournu, H., Peters, T.L. & Palmer, G.E. Endosomal Trafficking Defects Can Induce Calcium-Dependent Azole Tolerance in *Candida albicans*. *Antimicrob Agents Chemother* **60**, 7170-7177 (2016).

107. Hameed, S., Dhamgaye, S., Singh, A., Goswami, S.K. & Prasad, R. Calcineurin signaling and membrane lipid homeostasis regulates iron mediated multidrug resistance mechanisms in *Candida albicans*. *PLoS One* **6**, e18684 (2011).

108. Park, Y.N. & Morschhauser, J. Tetracycline-inducible gene expression and gene deletion in *Candida albicans*. *Eukaryot Cell* **4**, 1328-42 (2005).

109. Weyler, M. & Morschhauser, J. Tetracycline-inducible gene expression in *Candida albicans*. *Methods Mol Biol* **845**, 201-10 (2012).

110. Xie, J.L. *et al.* The *Candida albicans* transcription factor Cas5 couples stress responses, drug resistance and cell cycle regulation. *Nat Commun* **8**, 499 (2017).

111. CLSI. Method for Antifungal Disk Diffusion Susceptiplity Testing of Yeasts; Approved Guideline-Second Edition. *CLSI document M27-S4. Wayne: Clinical and Laboratory Standards Institute* (2009).

112. Redding, S.W. *et al.* Variations in fluconazole susceptibility and DNA subtyping of multiple *Candida albicans* colonies from patients with AIDS and oral candidiasis suffering one or more episodes of infection. *J Clin Microbiol* **35**, 1761-5 (1997).

1000

1001

1002 **Clearing the Fungal FoG: Perseverance, a property distinct from resistance, is**

1003 **associated with clinical persistence**

1004

1005 Alexander Rosenberg[1*], Iuliana V. Ene[2*], Alon M. Dahan[1], Ella Shtifman Segal[1],

1006 Arnaldo L. Colombo[3], Richard J. Bennett[2], Judith Berman[1**]

1007

1008

1009

1010 **Supplementary Material**

1011

1012

1013

1014 **Table of contents**

1015 Supplementary text ……..…….....3

1016 Summary of lineage changes in lab strains derived from SC5314…….....4-6

1017 Supplementary references …….…….…..7

1018 Supplementary Figure 1 ……..…….....….8

1019 Supplementary Figure 2 ……..…….…….....….9

1020 Supplementary Figure 3 ……..…….…...…..10-11

1021 Supplementary Figure 4 ……..…….…….....…12

1022 Supplementary Figure 5 ……..…….…….....…13

1023 Supplementary Figure 6 ……..…….…….....….14

1024 Supplementary Figure 7 ……..…….…….....15-16

1025 Supplementary Figure 8 ……..…….…….....….17

1026 Supplementary Table 2 ..…….…….....18

1027 Supplementary Table 3 ……..……..…...19

1028 Supplementary Table 4 ……..……..…...20

1029 Supplementary videos …….…..21

1030

1031

1032

1033

1034

1035

1036

1037

1038

1039

1040

1041

1042 **Supplementary text** (describing parental strains in Supplementary Fig. 8)

1043 Lab strain CAI-4 differs from SC5314 in that both copies of *URA3* and the adjacent
1044 gene, *IRO1,* were sequentially deleted[1,2]. In addition, the strain had undergone several
1045 homozygosis events[3]. Transformation of CAI-4 with *URA3* (Supplementary Table 2, CAI-
1046 4+*URA3*) did not restore FoG to SC5314 levels, but introduction of a single copy of both
1047 *URA3* and *IRO1* into derivative SN76 was sufficient to restore FoG to SC5314 levels
1048 (Supplementary Fig. 8 and Supplementary Table 2, SN95). This suggests that deletion of
1049 *IRO1* is responsible for a difference in perseverance levels in many derivatives of SC5314
1050 and that different LOH events did not affect FoG levels, although we note that the
1051 hemizygosity acquired in BWP17[4] may have contributed to the exceptionally low
1052 perseverance levels in this specific strain (Supplementary Fig. 8 and Supplementary Table
1053 2). Indeed, deletion of *IRO1* alone in strain SN152 (*MTLa*/*MTL*Δ*)* reduced FoG to levels
1054 similar to those seen in derivatives of CAI-4 (Supplementary Fig. 8A,B). Thus, deletion of
1055 *IRO1* in most lab strains is sufficient to explain the reduced FoG in these strains.
1056 Accordingly, all analysis of mutant isolates are presented relative to the isogenic parental
1057 strain from which they were derived.
1058
1059
1060
1061
1062
1063
1064
1065
1066
1067
1068
1069

1070 **Summary of lineage changes in lab strains derived from SC5314:**

1071 **SC5314**

1072 **CAF2-1** (derived from SC5314)

1073 LOH to: allele A @ Chr7L near CEN

1074 **CAI4** (derived from CAF-2)

1075 *ura3*Δ/Δ *iro1*Δ/Δ

1076 LOH to: allele A @ Chr7L near CEN;

1077 LOH to: allele B @ Chr3R near CEN;

1078 Trisomy of: Chr1 &/or 2

1079 **RM10** (derived from CAI-4)

1080 *his1*Δ/+ *ura3*Δ/Δ *iro1*Δ/Δ

1081 LOH to: allele A @ Chr2L;

1082 LOH to: allele A @ Chr7L near CEN;

1083 LOH to: allele B @ Chr3R near CEN;

1084 Trisomy of: Chr2

1085 **RM100#13** (derived from RM10)

1086 *his1*Δ/+ *ura3*Δ/+ *iro1*Δ/Δ

1087 Monosomy of Chr5 terminal 30 kb allele A

1088 LOH to: allele A @ Chr2L

1089 LOH to: allele A @ Chr7L near CEN

1090 LOH to: allele B @ Chr3R near CEN

1091 **RM1000#6** (derived from RM100)

1092 *his1*Δ/Δ *ura3*Δ/Δ *iro1*Δ/Δ

1093 Monosomy of Chr5 terminal 30 kb allele A

1094 LOH to allele B @ Chr3R near CEN

1095 LOH to: allele A @ Chr2L

1096 LOH to: allele A @ Chr7L near CEN

1097 **BWP17** (derived from RM1000#6)

1098 *his1*Δ/Δ *ura3*Δ/Δ *iro1*Δ/Δ *arg4*Δ/Δ

1099 LOH to: allele A @ Chr2L

1100 LOH to: allele B @ Chr3R near CEN

1101 LOH to: allele A @ Chr4 near right telomere

1102 LOH to: allele A @ Chr7L near CEN

1103 Monosomy of Chr5 terminal 30 kb allele A

1104 **SN76 or RM1000#2** (derived from RM100)

1105 *his1*Δ/Δ *ura3*Δ/Δ *iro1*Δ/Δ

1106 Homozygosis of Chr5 terminal 30 kb to disomic allele A

1107 LOH to: allele B @ Chr3R near CEN

1108 LOH to: allele A @ Chr2L

1109 LOH to: allele A @ Chr7L near CEN

1110 **SN95** (derived from SN76)

1111 *MTLa/alpha his1*Δ/Δ *ura3*Δ/+ *iro1*Δ/+ *arg4*Δ/Δ

1112 Homozygosis of Chr5 terminal 30 kb to disomic allele A

1113 LOH to: allele B @ Chr3R near CEN

1114 LOH to: allele A @ Chr2L

1115 LOH to: allele A @ Chr7L near CEN

1116 **SN152*** (derived from SN95)

1117 *MTLa*/Δ *leu2*Δ/+ *his1*Δ/+ *ura3*Δ/+ *iro1*Δ/+ *arg4*Δ/+

1118 Homozygosis of Chr5 terminal 30 kb to disomic allele A

1119 LOH to: allele B @ Chr3R near CEN

1120 LOH to: allele A @ Chr2L

1121 LOH to: allele A @ Chr7L near CEN

1122 ***SN152 iro1*Δ*** (derived from SN152)

1123 *MTLa*/Δ *leu2*Δ/+ *his1*Δ/+ *ura3*Δ/+ *iro1*Δ/Δ *arg4*Δ/+

1124 Homozygosis of Chr5 terminal 30 kb to disomic allele A

1125 LOH to: allele B @ Chr3R near CEN

1126 LOH to: allele A @ Chr2L

1127 LOH to: allele A @ Chr7L near CEN

1128 **Not sequenced to detect additional possible LOH events*

1129

1130

1131

1132

1133

1134

1135

1136

1137

1138

1139

1140

1141

1142

1143

1144

1145

1146

1147

1148

1149

1150

1151

1152

1153

1154 **Supplementary references**

1155 1. Fonzi, W.A. & Irwin, M.Y. Isogenic strain construction and gene mapping in *Candida*
1156 *albicans*. *Genetics* **134**, 717-728 (1993).

1157 2. Noble, S.M. & Johnson, A.D. Strains and strategies for large-scale gene deletion
1158 studies of the diploid human fungal pathogen *Candida albicans*. *Eukaryot Cell* **4**,
1159 298-309 (2005).

1160 3. Abbey, D., Hickman, M., Gresham, D. & Berman, J. High-Resolution SNP/CGH
1161 Microarrays Reveal the Accumulation of Loss of Heterozygosity in Commonly Used
1162 *Candida albicans* Strains. *G3 (Bethesda)* **1**, 523-30 (2011).

1163 4. Selmecki, A., Bergmann, S. & Berman, J. Comparative genome hybridization reveals
1164 widespread aneuploidy in *Candida albicans* laboratory strains. *Mol Microbiol* **55**,
1165 1553-65 (2005).

1166 5. Alby, K. & Bennett, R.J. Stress-induced phenotypic switching in *Candida albicans*.
1167 *Molecular biology of the cell* **20**, 3178-3191 (2009).

1168 6. Bensen, E.S., Clemente-Blanco, A., Finley, K.R., Correa-Bordes, J. & Berman, J.
1169 The mitotic cyclins Clb2p and Clb4p affect morphogenesis in *Candida albicans*. *Mol*
1170 *Biol Cell* **16**, 3387-400 (2005).

1171 7. Redding, S.W. *et al.* Variations in fluconazole susceptibility and DNA subtyping of
1172 multiple *Candida albicans* colonies from patients with AIDS and oral candidiasis
1173 suffering one or more episodes of infection. *J Clin Microbiol* **35**, 1761-5 (1997).

1174

Supplementary Figure 1

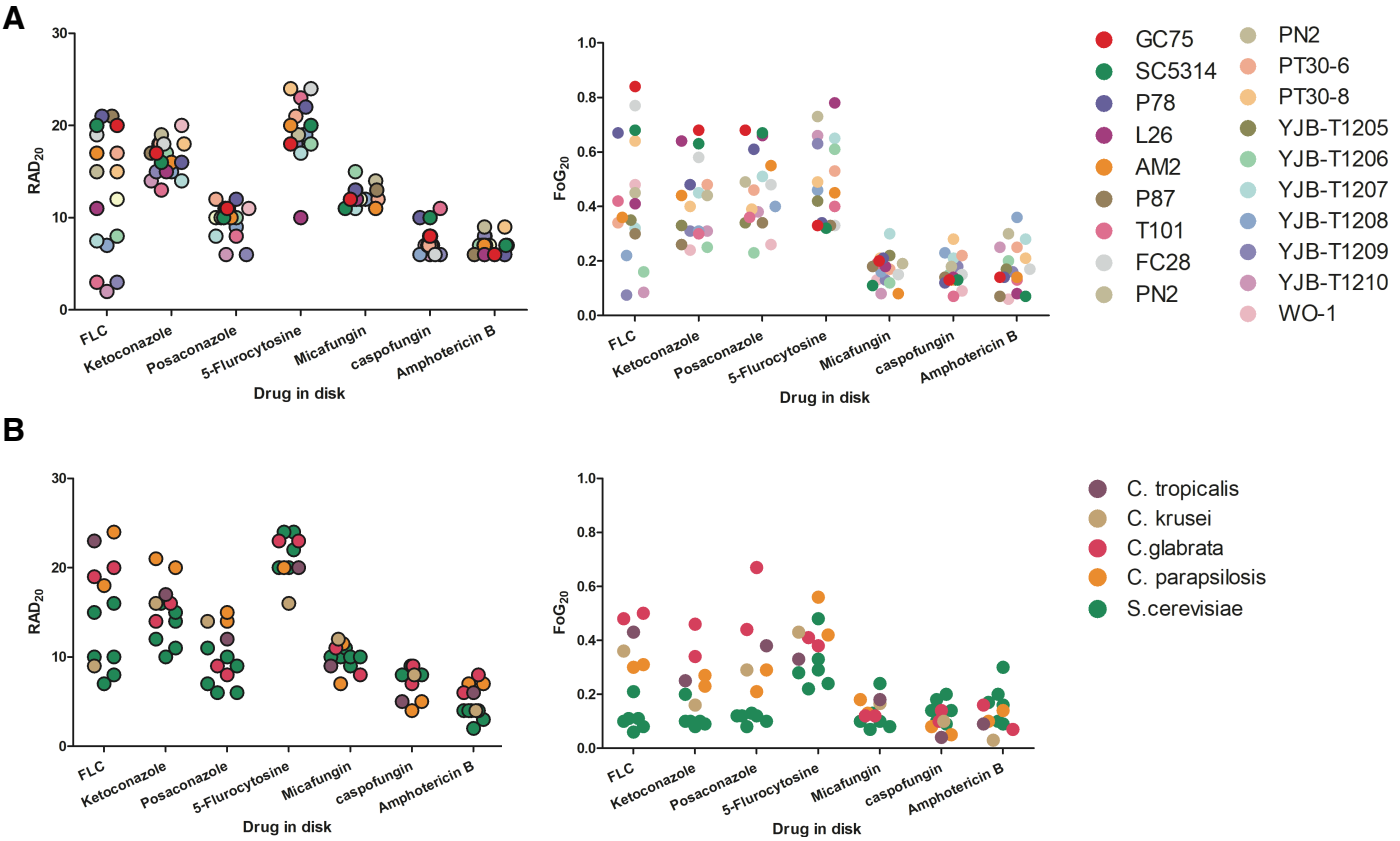

Supplementary Figure 1. Perseverance is detected for different drugs and fungal species. (a) Disk diffusion assays measure RAD and FoG levels for a set of 19 *C. albicans* isolates in response to diverse antifungal drugs containing fluconazole (25 µg), ketoconazole (10 µg), poseconazole (10 µg), 5-fluorocytosine (25 µg), micafungin (5 µg), caspofungin (5 µg), or amphotericin B (50 µg). (b) Disk diffusion assays performed with 25 µg fluconazole disks detect RAD and FoG levels for different pathogenic yeast species including *C. tropicalis*, *C. krusei*, *C. glabrata*, *C. parapsilosis* and *S. cerevisiae*. Note that FoG levels in azoles were particularly low for *S. cerevisiae.*

Supplementary Figure 2

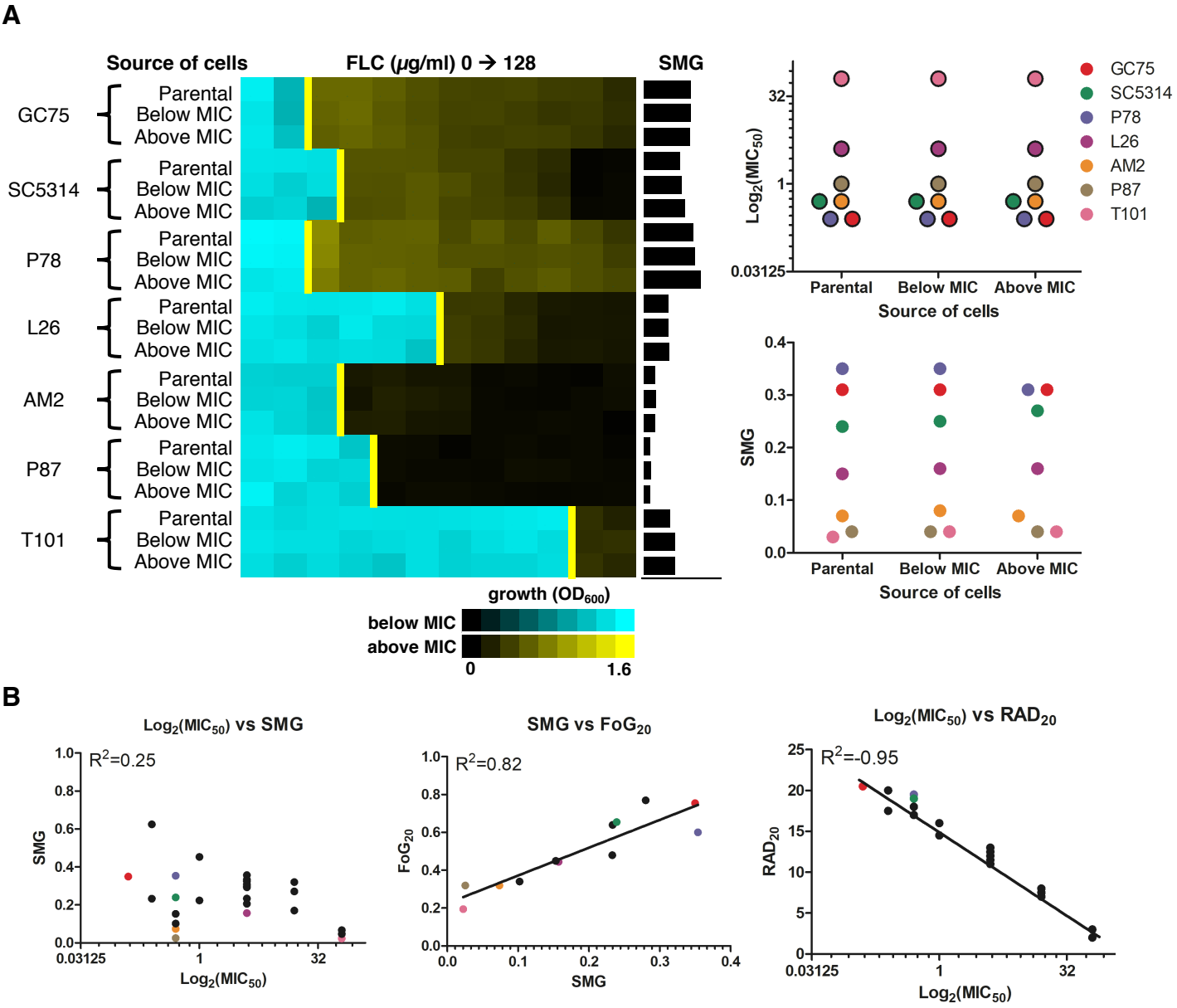

Supplementary Figure 2. Measuring drug responses of *C. albicans* isolates using broth microdilution assays (BMDAs). (a) Comparison of MIC and SMG for parental isolates compared with progeny from wells with drug concentration below (cyan heatmaps) or above (yellow heatmaps) the MIC_{50} (yellow lines) are very similar. MIC_{50}, (top right) and SMG (lower right) levels are similar for parental and progeny cells. (b) Correlation analyses for $log_2(MIC_{50})$ vs SMG (n-28, *P*-0.0064) , SMG vs FoG_{20} (n-12, *P*<0.0001), $log_2(MIC_{50})$ vs RAD_{20} (n-28, *P*<0.0001) for the series of isolates analyzed in Figure 1.

Supplementary Figure 3

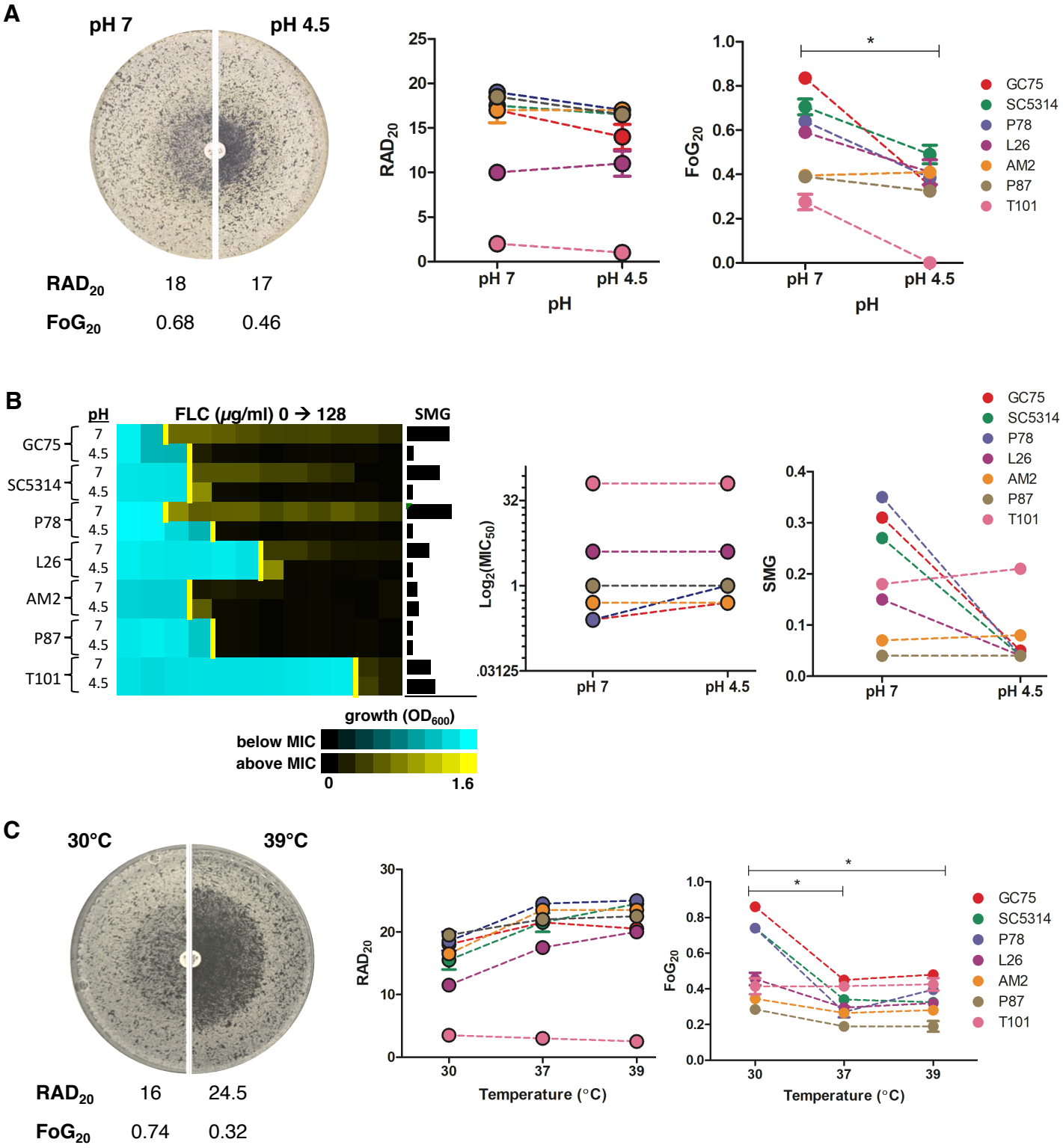

Supplementary Figure 3, continued

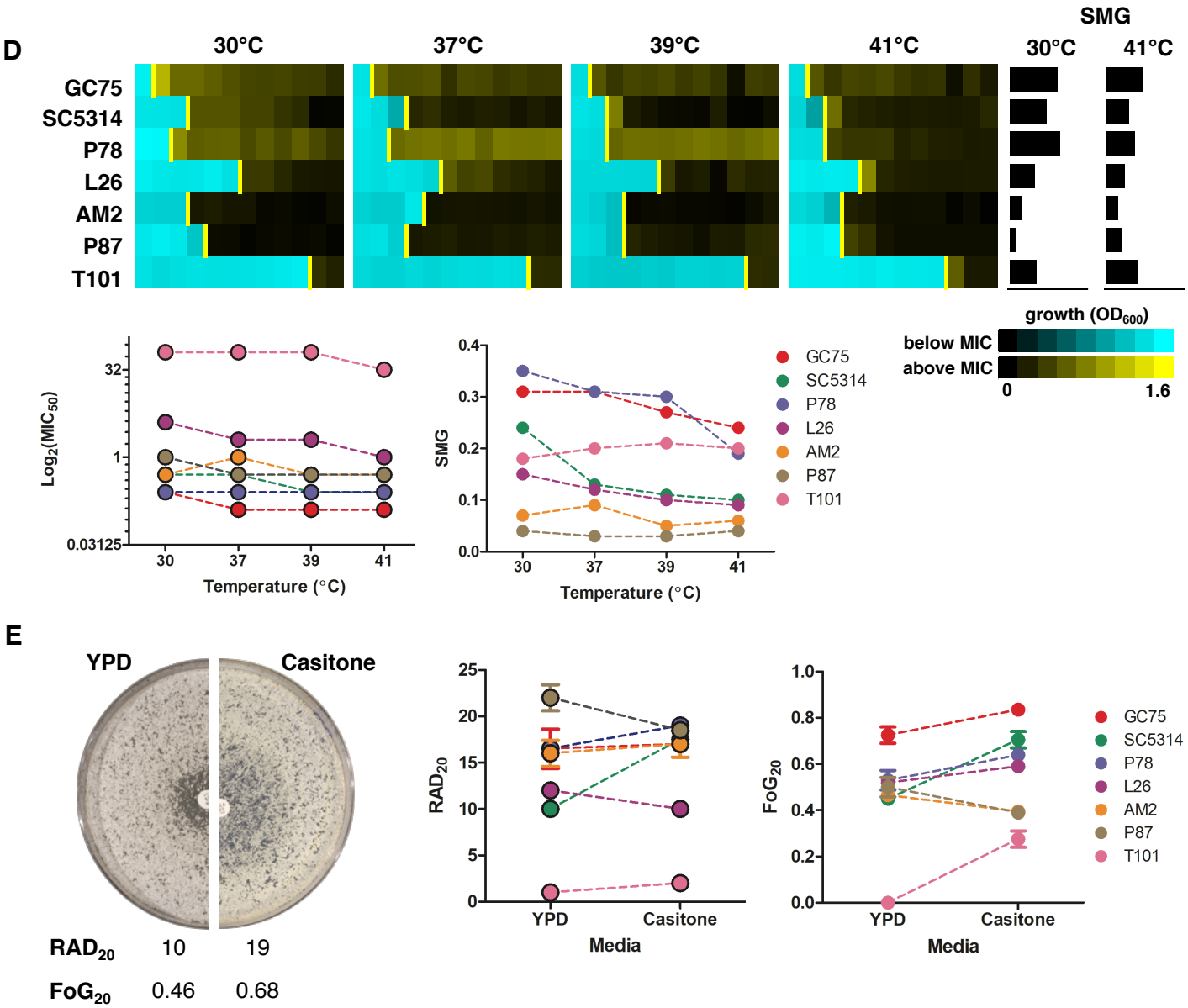

Supplementary Figure 3. Impact of growth conditions on FoG and SMG levels.
Disk diffusion assays (a,c,e) and broth microdilution assays (b,d) measure effect of different pH (a,b) (RAD (Paired t-test, t=2.2, df=6 n pairs=7, *P* - 0.0656), FoG (Paired t-test, t=3.4, df=6 n pairs=7, *P* - 0.0138), MIC (Paired t-test, t=1.33, df=6 n pairs=7, *P* – 0.2308) ,SMG (Paired t-test, t=2.3, df=6 n pairs=7, *P* – 0.0603)) temperature (c,d) (RAD (One way ANOVA, n groups=3, *P* - 0.6382), FoG (One way ANOVA, n groups=3, *P* - 0.0302) , MIC (One way ANOVA, n groups=4, *P* – 0.9646),SMG (One way ANOVA, n groups=4, *P* – 0.7366)) and nutrient media conditions (e) (RAD (Paired t-test, t=0.75, df=6 n pairs=7, *P* - 0.4797) FoG (Paired t-test, t=1.7, df=6 n pairs=7, *P* – 0.1491)) on RAD/MIC and FoG/SMG levels. Disk diffusion assays performed with strain SC5314 (left panels), RAD levels (middle panels) and FoG levels (right panels) calculated with for range of *C. albicans* strains as in Figure 1. Broth microdilution assays were analyzed as in Figure 2 for the same set of strains in medium at pH 7 and pH 4.5 (b) and at 30, 37, 39 and 41°C (d).

Supplementary Figure 4

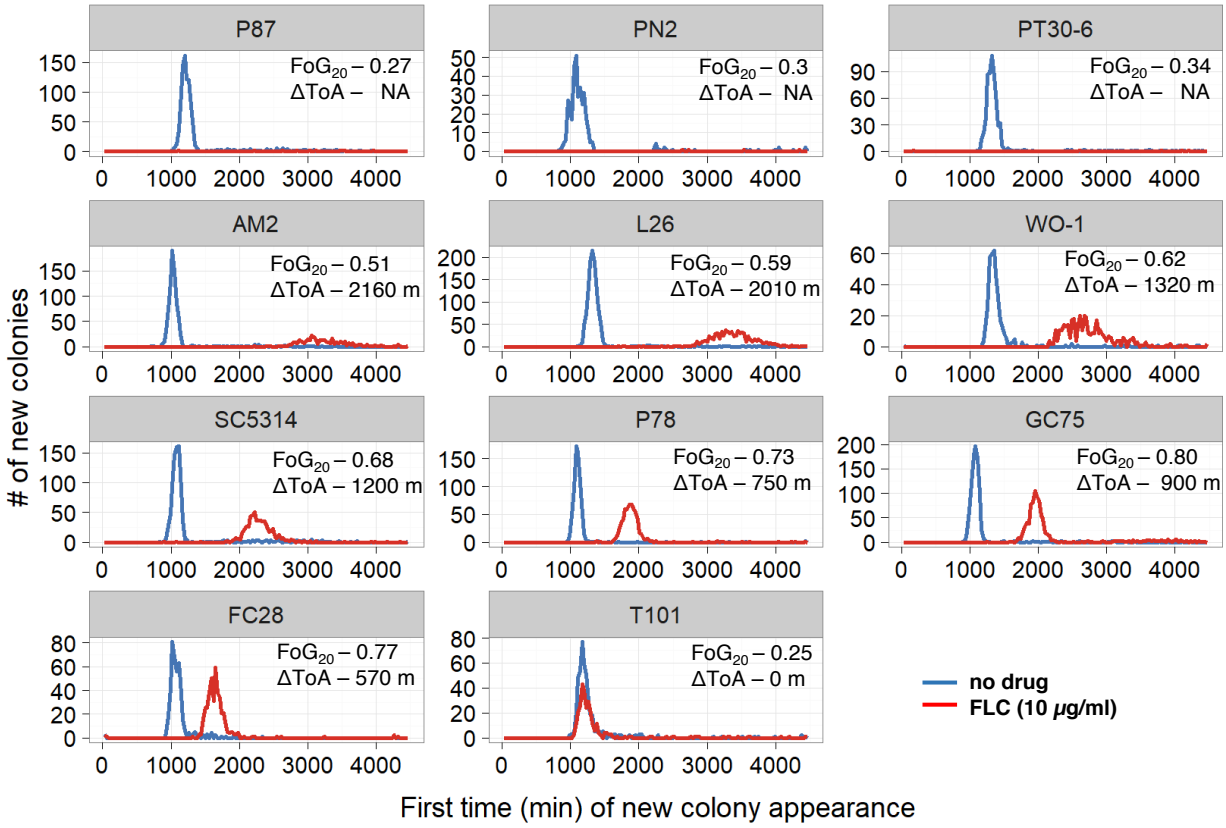

Supplementary Figure 4. Time of initial colony appearance (ToA) for strains with a range of FoG levels. ToA, determined using ScanLag, on a range of isolates with different FoG levels, as in Figure 4. Histograms show the time of new colony appearance and ΔToA indicates the difference in the time of appearance of colonies with vs without drug (ΔToA = ToA with 10 µg/ml fluconazole – ToA without fluconazole).

Supplementary Figure 5

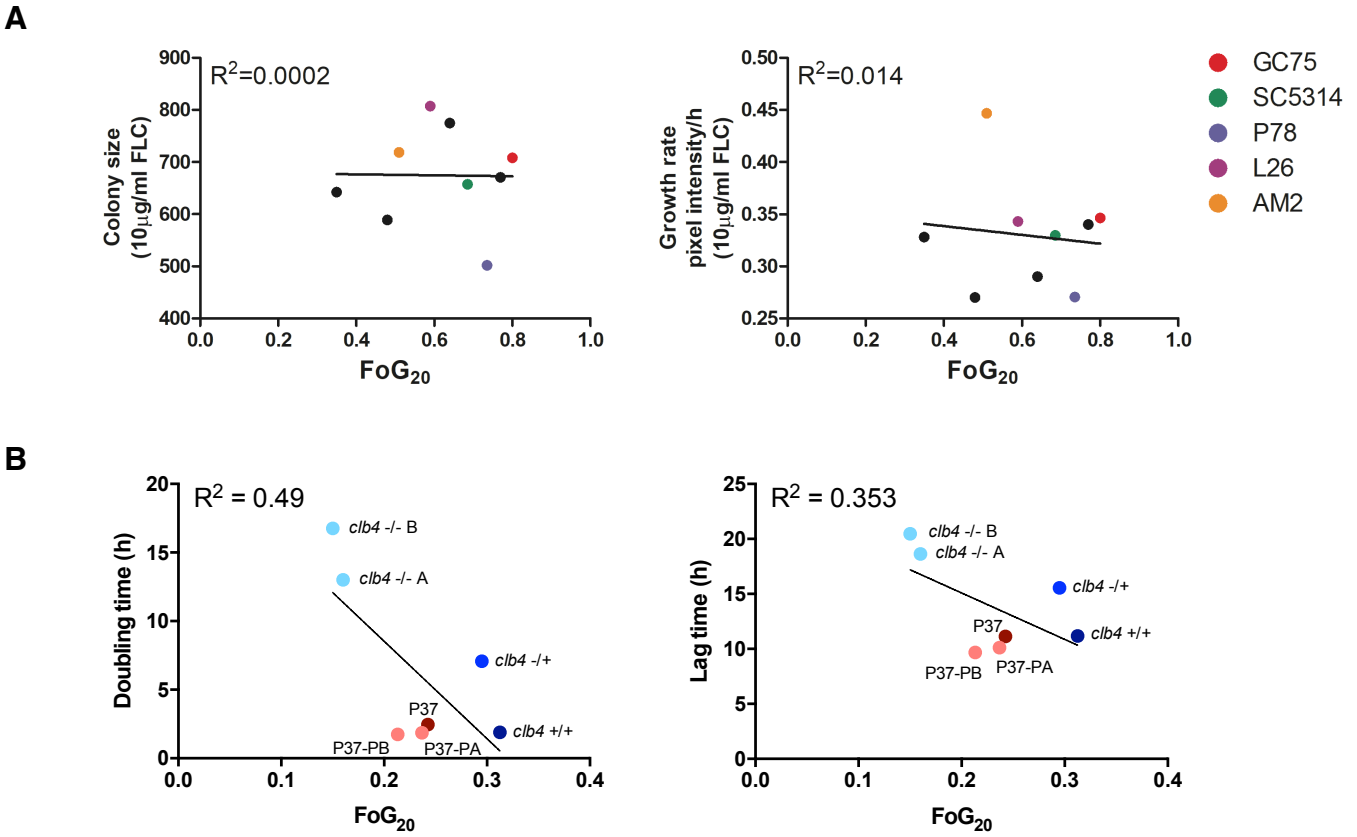

Supplementary Figure 5. Relationships between growth parameters and perseverance. (a) Correlation analyses for FoG and colony size (left) or FoG and growth rate (right) on casitone plates with 10 µg/ml fluconazole (n = 9). (b) Correlation analyses between FoG and doubling time or FoG and lag phase duration for related *C. albicans* isolates with differences in growth rates. Red data points indicate isolates from the P37055 lineage (P37 parental strain, and P37-PA,B passaged isolates[5]), blue data points indicate isolates with different numbers of the mitotic cyclin *CLB4* gene (BWP17 *clb +/+*, *clb +/-*, *clb -/-* A,B[6]). Data points represent the average of 3 biological replicates (n = 3, $P = 0.075$ for FoG vs Doubling time, $P = 0.16$ for FoG vs Lag time).

Supplementary Figure 6

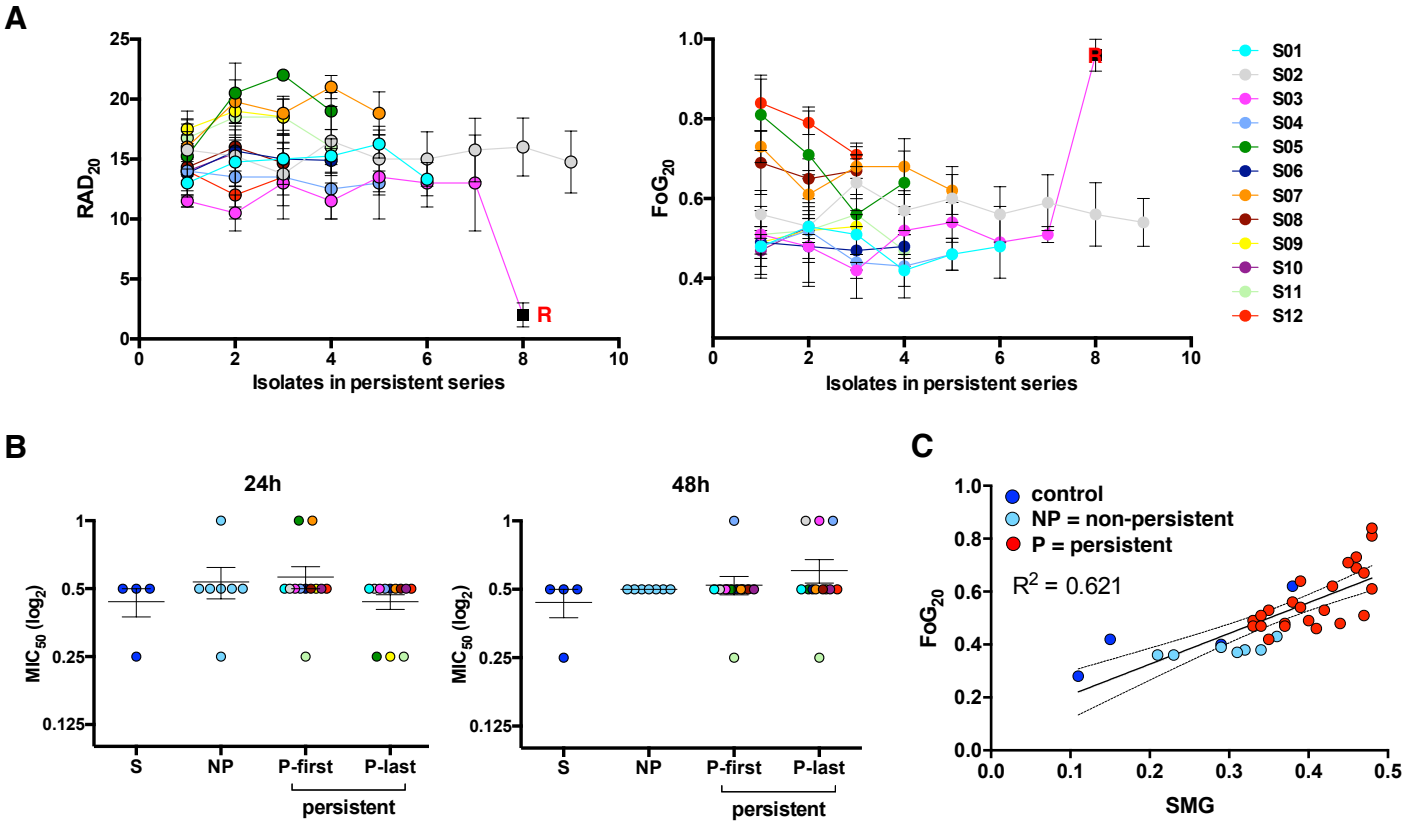

Supplementary Figure 6. FoG and SMG levels differ between persistent and non-persistent clinical isolates. (a) Fluconazole disk diffusion assays performed on all isolates from each patient series with a clinically persistent infection (Figure 5A) were analyzed using *diskImageR* for RAD (left) and FoG (right). The final isolate in the S03 series became resistant during therapy and is shown in a black square (R). (b) 24 and 48 h MIC levels from BMDAs for drug-susceptible isolates (SC5314, GC75, P78042 and P87), non-persistent isolates (NP1-7), and the first and the last isolate in each of the 12 persistent series (S01-12). The final isolate in S03 became fluconazole resistant (R), therefore the penultimate isolate in this series was included. (c) Correlation analysis between FoG and SMG levels for susceptible control strains (dark blue), persistent (red) and non-persistent isolates (light blue) (n = 35, $P < 0.0001$).

Supplementary Figure 7

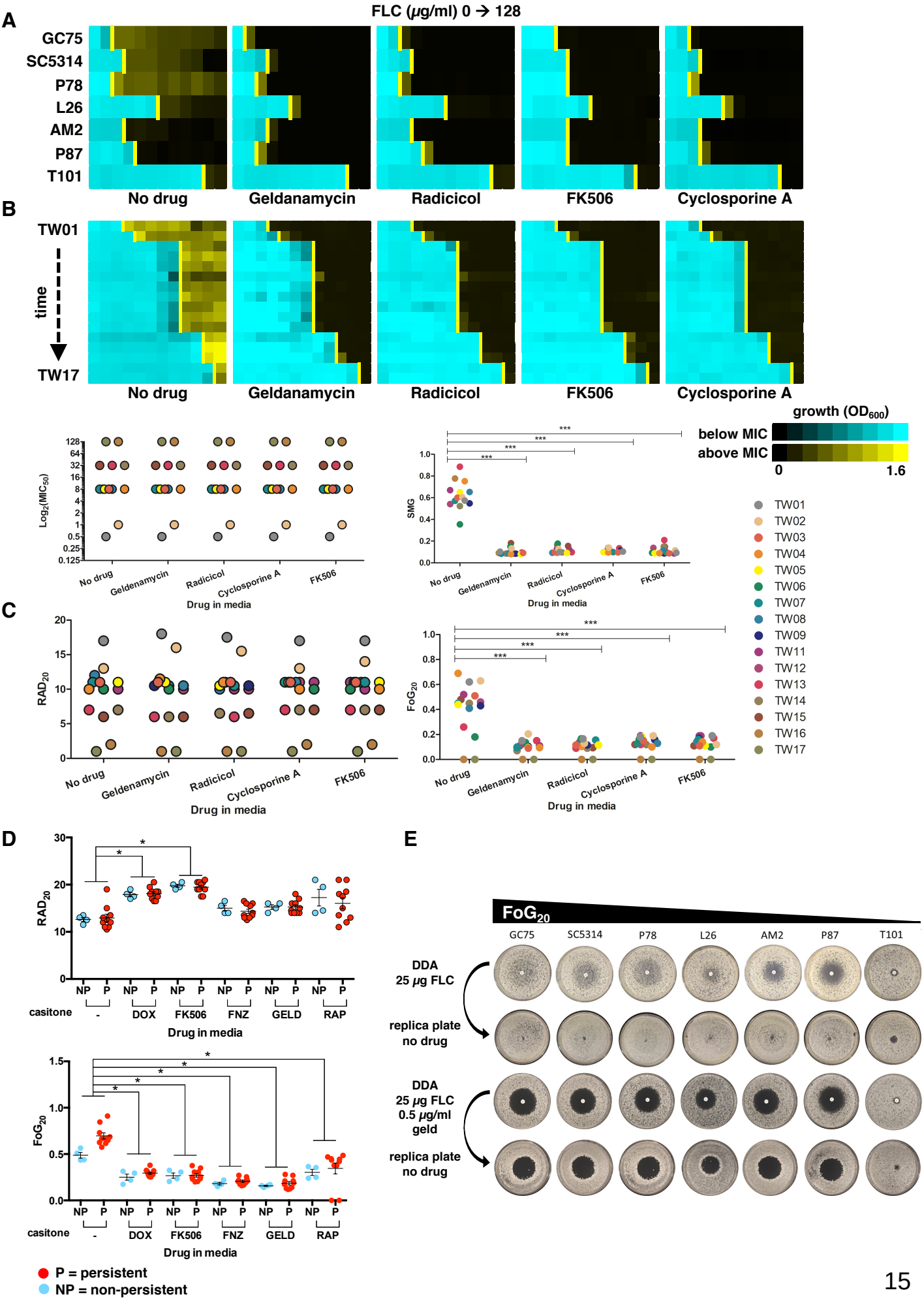

Supplementary Figure 7. Fluconazole adjuvants significantly reduce perseverance. (a,b) Broth-micro dilution assays on casitone media supplemented with 0.5 µg/ml geldanamycin, 0.5 µg/ml radicicol, 0.5 µg/ml FK506 or 0.4 µg/ml cyclosporine A for 7 *C. albicans* isolates (a) and a clinical isolate series[7] isolated from a single HIV patient (b). MIC_{50} values (yellow bars) were calculated as the fluconazole concentration resulting in 50% growth inhibition relative to wells with no fluconazole. Cyan heatmaps indicate growth below MIC, while yellow heatmaps indicate growth above MIC levels. Graphs show MIC (1-way ANOVA, n groups=5 , P- 1) and SMG (1-way ANOVA, n groups=5 , $P < 0.0001$) levels for the 16 isolates in the HIV series[7]. (c) RAD and FoG levels from fluconazole disk diffusion assays performed on casitone media supplemented with Hsp90 inhibitors (0.5 µg/ml geldanamycin or 0.5 µg/ml radicicol) or calcineurin inhibitors (0.5 µg/ml FK506 or 0.4 µg/ml cyclosporine A) on the series of 16 clinical isolates from a single HIV patient and analyzed using *diskImageR.* RAD (1-way ANOVA, n groups=5 , P- 0.9999) and FoG (1-way ANOVA, n groups=5 , $P < 0.0001$) levels. (d) Fluconazole disk diffusion assays for a subset of non-persistent (NP, n = 4, cyan dots) and persistent (P, n = 10, red dots) isolates from Figure 5 measured at 48 h on casitone media supplemented with adjuvant drugs (doxycycline 50 µg/ml, 0.5 µg/ml FK506, 10 µg/ml fluphenazine, 0.5 µg/ml geldanamycin or 0.5 ng/ml rapamycin) (for RAD $P < 0.001$ for no drug vs DOX and no drug vs FK506, $p > 0.05$ for the other drugs; for FoG $P < 0.01$ for all drug comparisons). (e) Effect of geldanamycin on viability of cells growing in the ZOI. fluconazole disk diffusion assays on casitone media (top two rows, as in Figure 3) or casitone medium supplemented with 0.5 µg/ml geldanamycin (bottom two rows), were replica-plated onto casitone plates without drug and incubated at 30°C for 48 h.

Supplementary Figure 8

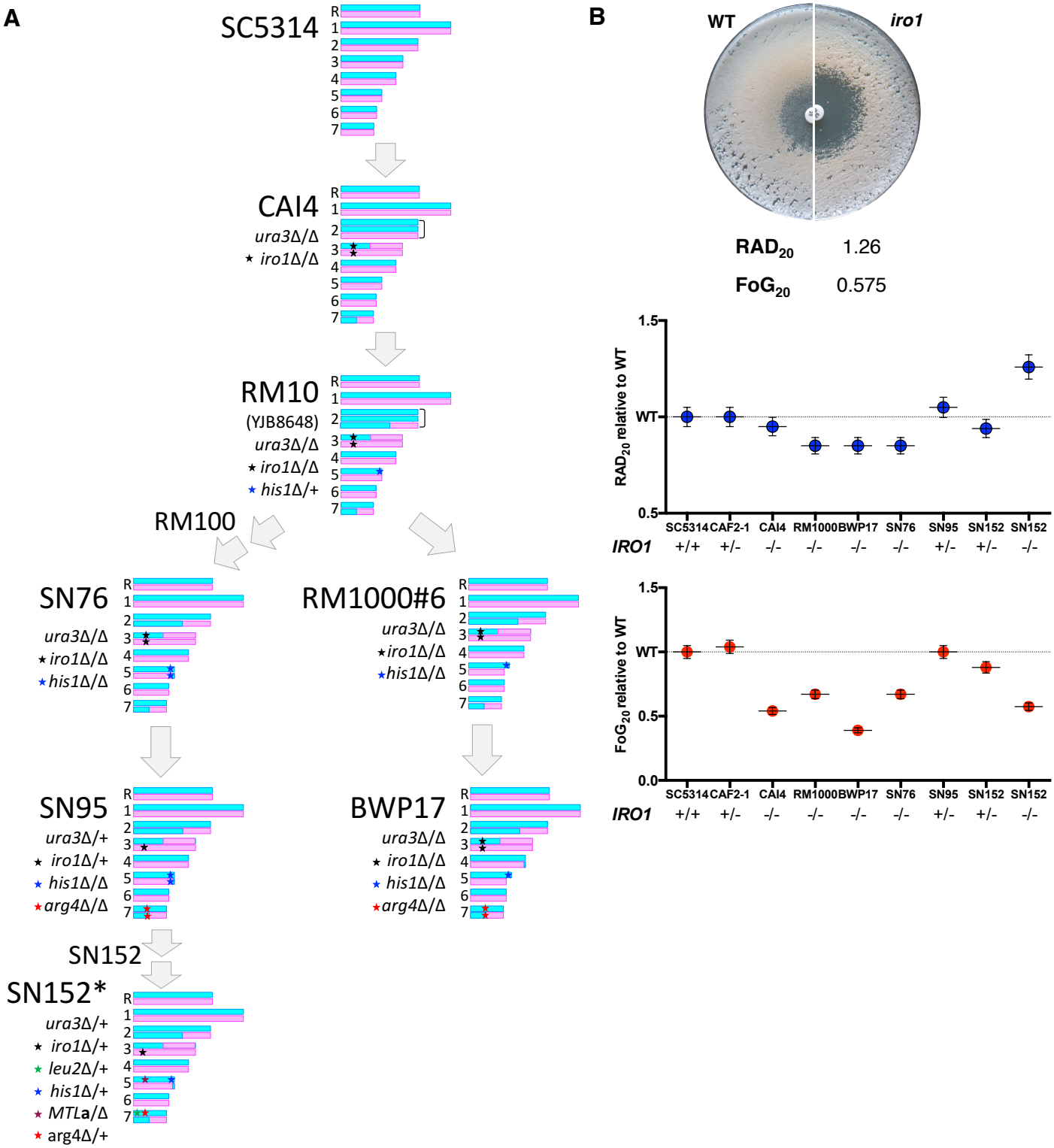

Supplementary Figure 8. Impact of *IRO1* on FoG levels in a standard laboratory lineage. (a) Cartoon of the SC5314 lineage and its derivatives CAF2-1, CAI4, RM10, RM1000, BWP17, SN76, SN95, and SN152 strain containing one or no *IRO1* alleles present (stars indicate location of deleted genes on the respective chromosomes). (b) Fluconazole disk diffusion assays performed using a series of laboratory strains in which the *IRO1* gene was inadvertent deleted or reintegrated. +/- signs indicate presence or absence of *IRO1* (+/+, both *IRO1* alleles present, +/-, one *IRO1* allele present, -/- no *IRO1* alleles present). RAD and FoG levels are shown relative to the most ancestral isolate in the lineage (SC5314). Pictures show fluconazole disk assays performed on an *iro1* null mutant and corresponding parental strain. Histograms show RAD (middle panel) and FoG (right panel) for strains SC5314, CAF2-1, CAI4, RM1000, BWP17, SN76, SN95, and 2 versions of the SN152 strain containing one or no *IRO1* alleles present (n = 2).

Supplementary Table 2

Strain	Casitone		*URA3*	*IRO1*	FoG responsive to Ca2+
	RAD_{20}	FoG_{20}			
SC5314	1.00	1.00	*ura3+/+*	*iro+/+*	yes
CAF2-1	1.00	1.04	*ura3+/-*	*iro+/-*	yes
CAI4	0.95	0.54	*ura3-/-*	*iro-/-*	no
CAI4 + *URA3*	0.95	0.54	*ura3-/-*	*iro-/-*	yes
RM1000 #6	0.85	0.67	*ura3-/-*	*iro-/-*	yes
BWP17	0.85	0.39	*ura3-/-*	*iro-/-*	yes
RM1000 #2	0.90	0.70	*ura3-/-*	*iro-/-*	yes
SN76	0.85	0.67	*ura3-/-*	*iro-/-*	yes
SN95	1.05	1.00	*ura3+/-*	*iro+/-*	no
SN152*	1.13	0.94	*ura3+/-*	*iro+/-*	yes
SN152* *iro1*Δ	1.26	0.57	*ura3+/-*	*iro-/-*	yes

Supplementary Table 2. RAD and FoG levels of SC5314-derived laboratory strain lineage.

Supplementary Table 3

Function/pathway tested	Relevant wild-type	Mutant	Casitone	
			RAD_{20}	FoG_{20}
calcinuerin pathway	SC5314	**SC5314**	1.00	1.00
		*cna1*ΔΔ	1.00	0.44
		*cnb1*ΔΔ	1.00	0.48
		*crz1*ΔΔ	1.00	0.50
	SN152	*crz1*ΔΔ	1.10	0.39
calcineurin regulators	SC5314	*rcn1*ΔΔ *crz1*ΔΔ	1.00	0.46
	SN95	*rcn1*ΔΔ	1.05	0.94
		*rcn2*ΔΔ	1.05	0.91
Calcium channels	SC5314	*mid1*ΔΔ	1.00	1.06
		*cch1*ΔΔ	1.00	1.03
vacuole/intracellular calcium concentration	CAI-4	**CAI4**	1.00	1.00
		*vps21*ΔΔ	1.00	2.34
cidality of fluconazole	SN152	**SN152**	1.00	1.00
		*cas5*ΔΔ	1.25	0.13
regulator of ergosterol biosynthesis genes	SN152	*upc2*ΔΔ	1.25	0.29
regulators of efflux pump genes		*tac1*ΔΔ	1.05	0.95
		*mrr1*ΔΔ	1.10	0.89
efflux pump genes	G5	**G5**	1.00	1.00
		*mdr1*ΔΔ	1.14	0.87
	CAI4	MDR1 OE	1.00	1.62
	SC5314	MDR-OE	1.00	0.92

Supplementary Table 3. RAD and FoG levels of null mutants of interest.

Supplementary Table 4

Primer	Sequence
BP1440	5' CCACTCCTTTTCCTTATTTCCCAAATCAACCAATTATTCTTTTTCTTACTCTTTA TTTGCgttttcccagtcacgacgtt 3'
BP1441	5' GTGATTGTAGGGGACGATACAAAATCTTGTTCTTTTTGTTTTTCATTAAGGAGA CCAGGCtgtggaattgtgagcggata 3'
BP1444	5' gtgctctccgcgacaatatctt 3'
BP1445	5' ccacgagacacgacctaataat 3'

Name	Plasmid	Reference
BJB-T2	pGEM-His1	Wilson *et al*., 1999
BJB-T61	pSN69-Arg4	Noble and Johnson, 2005

Supplementary Table 4. Plasmids and primers used in this study.

Supplementary Videos 1-3 . Time-lapse videos of cells from strains with similar MIC and different FoG levels. Cells were plated in liquid casitone medium containing 10µg/ml fluconazole, which is ~ 20-fold above their MIC levels. (1) Strain P87-low FoG (FoG-0.29, RAD-18), (2) Strain AM2- medium FoG (FoG-0.41, RAD-17) (3) SC5314- high FoG (FoG-0.68, RAD-18).